CHAPTER 7

SINGLE PHASE TO THREE-PHASE POWER CONVERSION

USING SPARSE CONVERTERS

7.1 Introduction

In the process of power conversion from single-phase to three-phase the concept of conventional circuits was discussed in the previous chapter. In this chapter converter topologies different from the conventional circuits named the 'Sparse Converters' are introduced and a detailed analysis of the mathematical model of the converters is laid down. These converters are used to simulate the energy conversion process using an induction machine as the load. The control scheme for the sparse converters to achieve unity power factor from the supply is also explained. Finally some simulation results obtained by simulating the sparse converters are presented.

7.2 Sparse Converters

This section considers the development of the sparse converters from the conventional converter topologies. The conventional single-phase to three-phase circuit as shown in Figure 7.1, consists of a single-phase full bridge ac-to-dc converter and a three-phase inverter. This circuit has five legs each being a series connection of two switching devices. A reactor is connected in series with the single-phase power supply and the input is applied between the central points of the full bridge ac-to-dc converter legs.
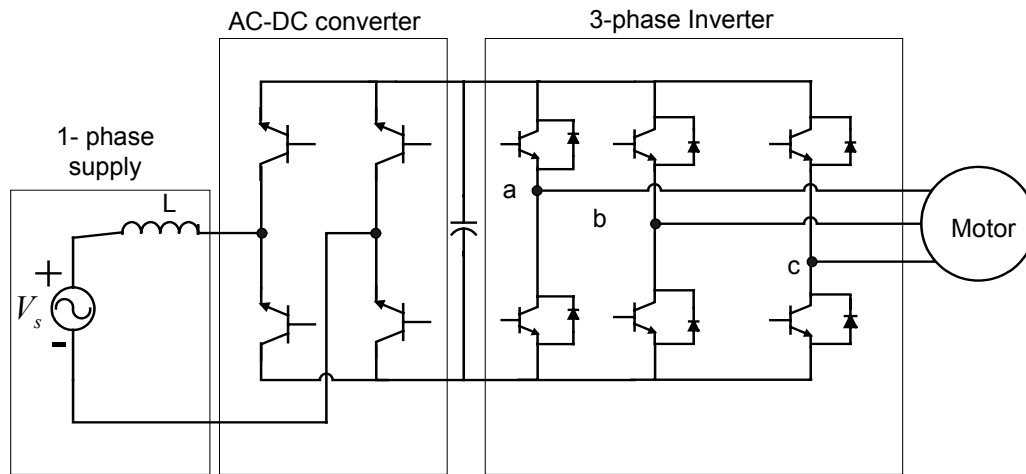
Figure 7.1: Conventional full-bridge ac/dc converter inverter circuit

The power supply current is controlled to be sinusoidal by the full-bridge ac-to-dc converter, while the motor input voltage is controlled by the pulse-width modulation inverter. These two control actions are independent and a capacitor is inserted for decoupling. To reduce the cost the full bridge converter can be replaced by a half-bridge converter in any case the input reactor is necessary which further increases the size of the system.

The three-phase inverter has eight switching states, which correspond to eight output voltage space vectors as shown in Table 7.1. Each state correspond to a voltage in each phase, but in particular there exists two states during which the inverter does not output any voltage on the phases. This happens when all the top devices or all the bottom devices are turned ON at the same time. These corresponding state vectors are referred to as zero vectors.

These zero vectors are equivalent in terms of generated line-to-line voltage, but differ in the induced voltage v_o between the neutral point of the star connected three phase load and the neutral point of the dc link, which is given as,

$$v_o = \frac{Vd}{2} \qquad \text{when all the top devices are on}$$

$$v_o = -\frac{Vd}{2} \qquad \text{when all the bottom devices are on}$$

Therefore the neutral point voltage of the load can be controlled by a proper use of the zero vectors. The model for the sparse converters is as shown in Figure 7.2. It consists of a motor, a three-phase inverter and an additional leg having the functionality of the ac-to-dc converter.

Table 7.1 The switching states in a three-phase inverter showing the zero voltage states.

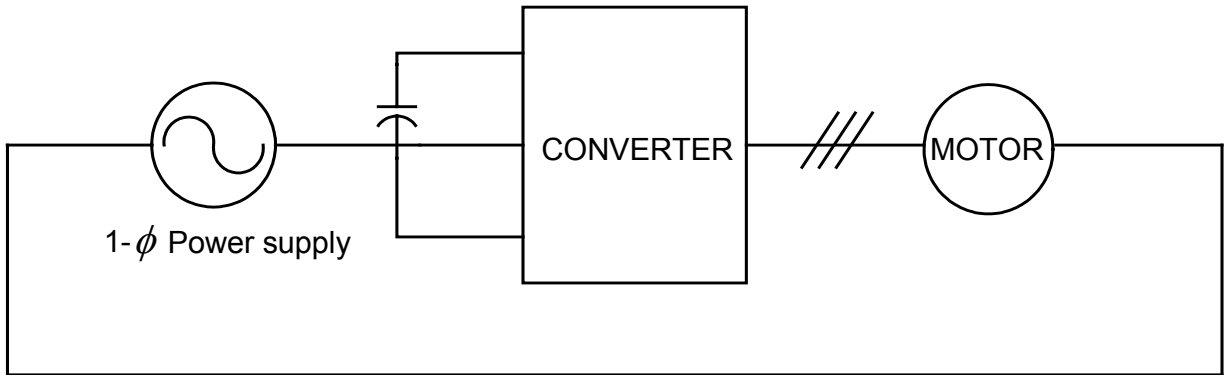| S_{11}	S_{12}	S_{31}	V_{ab}	V_{bc}	V_{ca}
0	**0**	**0**	**0**	**0**	**0**
0	0	1	0	$-V_{DC}$	V_{DC}
0	1	0	$-V_{DC}$	V_{DC}	0
0	1	1	$-V_{DC}$	0	$-V_{DC}$
1	0	0	V_{DC}	0	$-V_{DC}$
1	0	1	V_{DC}	$-V_{DC}$	0
1	1	0	0	V_{DC}	$-V_{DC}$
1	**1**	**1**	**0**	**0**	**0**

Figure 7.2: Model for Sparse converters.

The power supply is directly connected between the neutral point of the load, in doing so the input reactor as in conventional circuits becomes redundant as its purpose is served by the leakage inductance of the motor. Since the power supply is connected directly to the load, power supply current and the output voltage control actions are no longer independent as in the case of the conventional circuits. Owing to the connection of the power supply the load currents carry an additional amount of the current, which is one third of the supply current, and this current is the zero phase sequence current.

The zero-phase sequence current flowing in to the stator windings does not generate any torque and so therefore may be accepted as long as the related increase of copper losses is compensated by some advantages like the cost and size reduction [8].
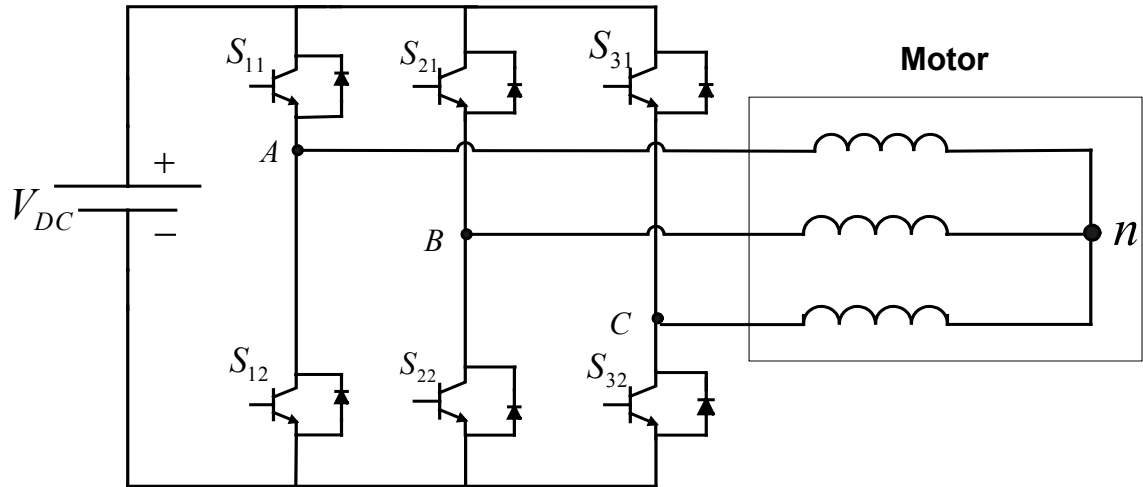
Figure 7.3: Positive-phase sequence equivalent circuit topology of the sparse converters

Figures 7.3 and 7.4 show the positive-phase sequence and the zero-sequence equivalent circuits of the sparse converters respectively. In the positive phase sequence circuit the power supply voltage does not appear since it is the zero-phase sequence voltage, and the equivalent circuit coincides with the conventional inverter topology. When considering the zero-phase sequence the motor is equivalent to a simple inductance and the inverter can be regarded as a single leg topology, the left leg of which is controlled as usual, while the right leg in Figure 7.4 is controlled by choosing the appropriate zero vector for the inverter.

Thus comparing the conventional converter with the sparse converters they both are equal when considering the leakage inductance of the motor as input reactance for the full bridge ac-to-dc converter. The equivalence is achieved in spite of the reduced number of switching devices and a very simple structure for the ac-to-dc converter is obtained.
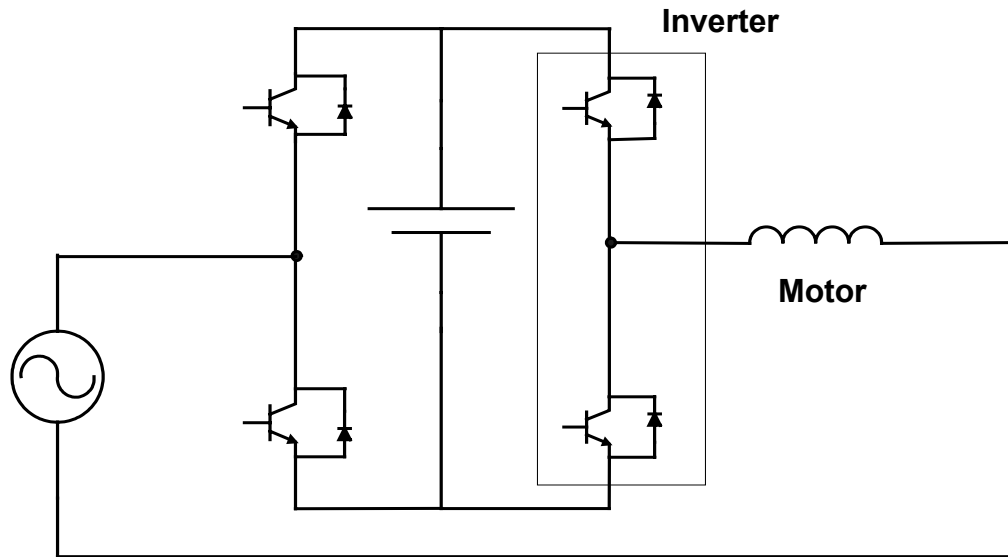
Figure 7.4: Zero-phase sequence equivalent circuit topology of the sparse converters

Since the sparse converters use the zero-phase sequence voltage to control the power supply current, it requires higher dc link voltage than the conventional circuits.

In this thesis three sparse converter topologies, Converter A, Converter B and Converter C, were modeled for an induction machine. An appropriate control scheme was set forth for each of them to achieve near to unity power factor form the supply and to regulate the speed of the induction machine.

7.3 Converter A

The model for the Converter A is shown in Figure 7.5. In this circuit the line side converter and the load side converter share a common capacitor leg. Two phases

(Phase 'A' and 'B') of the load are connected to the two switching legs where each leg consists of two switching devices, which operate such that if the top leg is on the bottom leg is off and vice-versa. The power supply is given directly to the neutral of the load. The switching devices are PWM operated in which the modulating signals obtained by calculation with in the control scheme are compared with a high frequency triangle to give the switching pulses to turn on or turn off the devices.
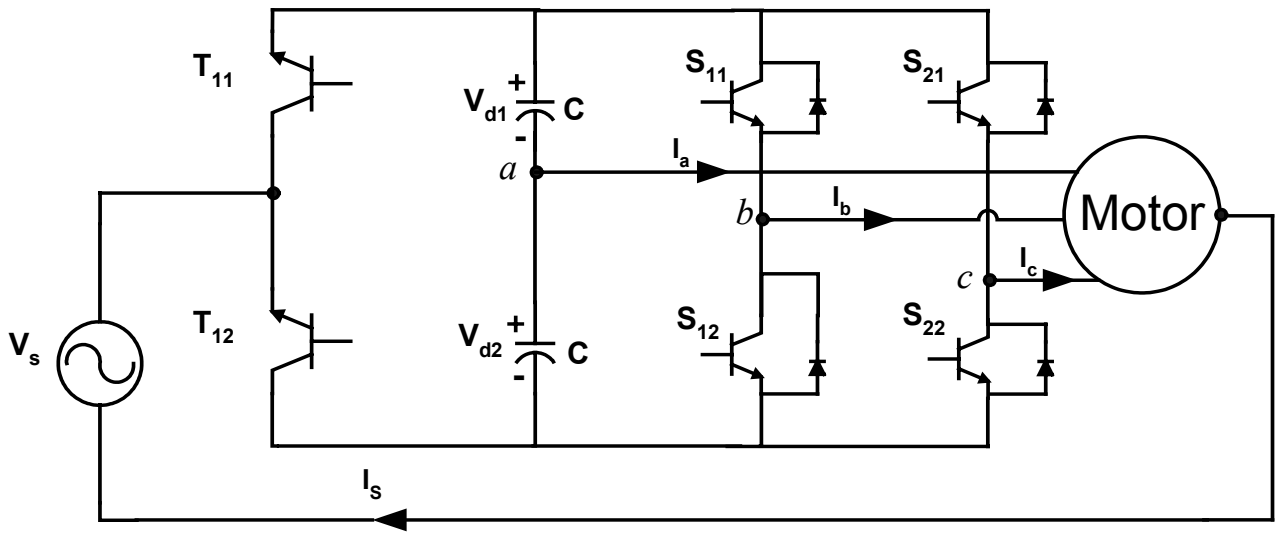

Figure 7.5: Model of sparse Converter A.

The model equations for Converter A are as follows,

$$V_{d2} = V_{an} + V_{nm} \tag{7.1}$$

$$V_d T_{21} = V_{bn} + V_{nm} \tag{7.2}$$

$$V_d T_{31} = V_{cn} + V_{nm} \tag{7.3}$$

V_{nm} is the voltage between the neutral point of the load to the DC link capacitor voltage as indicated in Fig 7.5. The voltages V_{an}, V_{bn}, V_{cn} are the inverter output voltage referred to the neutral point of the dc link and are expressed as

139

$$V_{an} = V_m \sin(\omega_e t) + v_o \qquad (7.4)$$

$$V_{bn} = V_m \sin(\omega_e t - 2\pi/3) + v_o \qquad (7.5)$$

$$V_{cn} = V_m \sin(\omega_e t + 2\pi/3) + v_o \qquad (7.6)$$

In Equations 7.4 through 7.6, V_m is the peak value of voltage, ω_e is the output frequency or the motor frequency and v_o is the zero-phase sequence voltage, which is the component of the supply voltage given as $v_o = v\sin(\omega_s t)$, with ω_s the supply frequency.

From Equation (7.1)

$$V_{mn} = V_{d2} - V_{an} \qquad (7.7)$$

The dc link capacitor voltage V_d is split into V_{d1} and V_{d2} whose sum gives the whole voltage and difference is the ripple (V_σ) that can be tolerated. The switching function for S_{21} and S_{31} can be expressed in terms of their modulation functions as,

$$S_{21} = \frac{1}{2}(1 + M_{21}) \qquad (7.8)$$

$$S_{31} = \frac{1}{2}(1 + M_{31}) \qquad (7.9)$$

so equations 7.2 and 7.3 can be written in terms of modulating signals as

$$M_{21} = \frac{1}{V_d}(2V_{bn} - 2V_{an} - V_\sigma) \qquad (7.10)$$

$$M_{31} = \frac{1}{V_d}(2V_{cn} - 2V_{an} - V_\sigma) \qquad (7.11)$$

The voltage V_{nn} depends on the switching of T_{11} and T_{21}, thus the modulating signal for these switches can be expressed as

$$M_{TT} = \frac{1}{V_d}(2V_s - 2V_{an} - V_\sigma) \tag{7.12}$$

where V_s is the power supply voltage.

M_{11} and M_{21} correspond to the modulation signals of the inverter legs and M_{tt} corresponds to the modulation signal for the converter leg. The modulating signals given in equations 7.10, 7.11 and 7.12 are compared with the high frequency triangle to get the pulses for the switching devices.

Kirchoff's current law (KCL) gives the current in the DC link capacitor as

$$CpV_d = 2T_{11}I_s - 2T_{21}I_b - 2T_{31}I_c - I_a \tag{7.13}$$

and $CpV_\sigma = I_a$, $\tag{7.14}$

where p is the differential operator with respect to time.

The currents I_a, I_b, I_c each contain one-third component of the supply current I_s. Thus the currents I_a, I_b, I_c can be expressed as,

$$I_a = I_{aa} + I_s/3 \tag{7.15}$$

$$I_b = I_{bb} + I_s/3 \tag{7.16}$$

$$I_c = I_{cc} + I_s/3, \tag{7.17}$$

where I_{aa}, I_{bb}, I_{cc} are the actual load currents and I_s is the supply current which is equal to

$$I_s = \frac{(I_{aa} + I_{bb} + I_{cc})}{3} \tag{7.18}$$

141

Due to the topology of the circuit the load currents contain one third of the supply current in each phase and the voltages contain a zero sequence component, which has the same frequency as that of the supply voltage (V_s) but the magnitude differs as explained in the above equations. The above equations model the converter while load modeling was already discussed in Chapter 3.

7.3.1 Control Scheme for Converter A

In deriving the equations for the control scheme it is often convenient to express the time varying quantities into time invariant ones, thus the above equations are transformed into a reference frame in which the control variables and the controlled variable are constants and in this case it is the synchronous reference frame. The control scheme for this converter is very similar to the conventional half-bridge converter with reduced switches as dealt with in Chapter 6. Due to the lack of control on phase 'a', the voltages of phases 'b' and 'c' (V_{bn}, V_{cn}) determine its voltage.

The load that is the induction machine is controlled to maintain a constant speed and rotor flux. The speed command and the flux command give the reference for the q-axis and the d-axis stator current respectively from which the q-axis and the d-axis stator voltages are found which are the actual outputs of the controller, that is the values of v_{qs} and v_{ds} are the reference voltages to be synthesized by the inverter.

The v_{qs} and v_{ds} obtained are converted back into abc frame using the frequency which is calculated by adding the rotor speed and the slip speed at very instant. This gives the three phase voltages (V_{an}, V_{bn}, V_{cn}) from which the modulation signals for the top and the bottom switching devices are found.

The switching signals are used to calculate the dc link voltage, which is compared with the reference to output the magnitude of the input supply current which adjusts to any changes in the load. For the supply voltage to be in phase with the supply current, the current is multiplied by the phase of the supply voltage, which is compared with the actual supply current, the difference is regulated to give the modulation signal for the line side converter. The actual supply current is obtained as the sum of the three load currents in accordance to the Equation 7.18. Thus in implementing the above control, speed and flux control of the induction machine and unity power factor from the supply is achieved.

As the capacitor is connected to phase 'a' only two modulation signals for the load side converter and for phase 'a' the modulation signal is constant or rather zero. Thus it is convenient to work with the voltages in this case rather than the modulation signals and so all the equations are expressed in terms of voltages and their transformed variables.

Since phase 'a ' is not controlled the modulation signal for phase 'a' can be written as

$$M_{11} = \frac{1}{V_d}(V_{an} - V_{an}) \tag{7.19}$$

The above equation along with Equations 7.10 and 7.11 can be written in matrix from as

$$\frac{V_d}{2}\begin{bmatrix} M_{11} \\ M_{21} \\ M_{31} \end{bmatrix} = \begin{bmatrix} V_{an} \\ V_{bn} \\ V_{cn} \end{bmatrix} - \begin{bmatrix} V_{an} \\ V_{an} \\ V_{an} \end{bmatrix} - \begin{bmatrix} 0 \\ V_\sigma \\ V_\sigma \end{bmatrix} \tag{7.20}$$

Transforming the above matrix into qdo frame the following equations are obtained

$$\frac{V_d}{2}\begin{bmatrix} m_{qs} \\ m_{ds} \\ m_{os} \end{bmatrix} = \begin{bmatrix} V_{qs} \\ V_{ds} \\ V_{os} \end{bmatrix} - \begin{bmatrix} \dfrac{V_\sigma}{2}\cos\theta_e \\ \dfrac{V_\sigma}{2}\cos\theta_e \\ V_{an} \end{bmatrix} - \begin{bmatrix} 0 \\ 0 \\ \dfrac{V_\sigma}{2} \end{bmatrix} \tag{7.21}$$

Thus from the above transformation

$$m_{qs} = \frac{(2V_{qs} + V_\sigma \cos\theta_e)}{V_d} \tag{7.22}$$

$$m_{ds} = \frac{(2V_{ds} + V_\sigma \cos\theta_e)}{V_d} \tag{7.23}$$

$$m_{os} = \frac{(2V_{os} - 2V_{an} - V_\sigma)}{V_d} \tag{7.24}$$

Equation 7.3 can be written in terms of modulation signals of phase 'b' and 'c' as

$$CpV_d = (I_s M_{tt} - I_b M_{21} - I_c M_{31}) \tag{7.25}$$

since $M_{11} = 0$ the above equation can be written as,

$$CpV_d = (I_s M_{tt} - I_a M_{11} - I_b M_{21} - I_c M_{31}) \tag{7.26}$$

transforming the above equation to qdo variables the current through the dc link capacitor becomes,

$$CpV_d = (I_s M_{tt} - I_{qs} m_{qs} - I_{ds} m_{ds} - 3I_{os} m_{os}) \tag{7.27}$$

and since the supply current is the zero-sequence current

$$I_{os} = \frac{I_s}{3} \qquad (7.28)$$

Thus, Equation 7.21 can now be written as

$$CpV_d = (I_s(M_{tt} - mos) - I_{qs}m_{qs} - I_{ds}m_{ds}) \qquad (7.29)$$

From Equation 7.12 and 7.24 the expression $(m_{tt} - m_{os})$ can be evaluated as

$$(m_{tt} - m_{os}) = \frac{2(V_s - v_{os})}{2} \qquad (7.30)$$

As M_{tt} and M_{os} are of the same frequency the term $(m_{tt} - m_{os})$ comprises of a constant term and a second harmonic term, and so Equation 7.29 is equivalent to,

$$(CpV_d + I_{qs}m_{qs} + I_{ds}m_{ds}) = I_s \qquad (7.31)$$

$$(CpV_d + I_{qs}\frac{m_{qs}}{V_d} + I_{ds}\frac{m_{ds}}{V_d}) = I_s \qquad (7.32)$$

where I_s is the fundamental component of supply current.

Considering all the equations derived till this point the overall control structure for the Converter A is as given in Figure 7.6.

7.3.2.Simualtion Results

The Converter A as shown in Figure 7.5 was simulated using Induction machine similar to the one used for the simulation of the conventional converters. The simulation results include some key parameters for the load and also show the actual quantities follow the reference values.
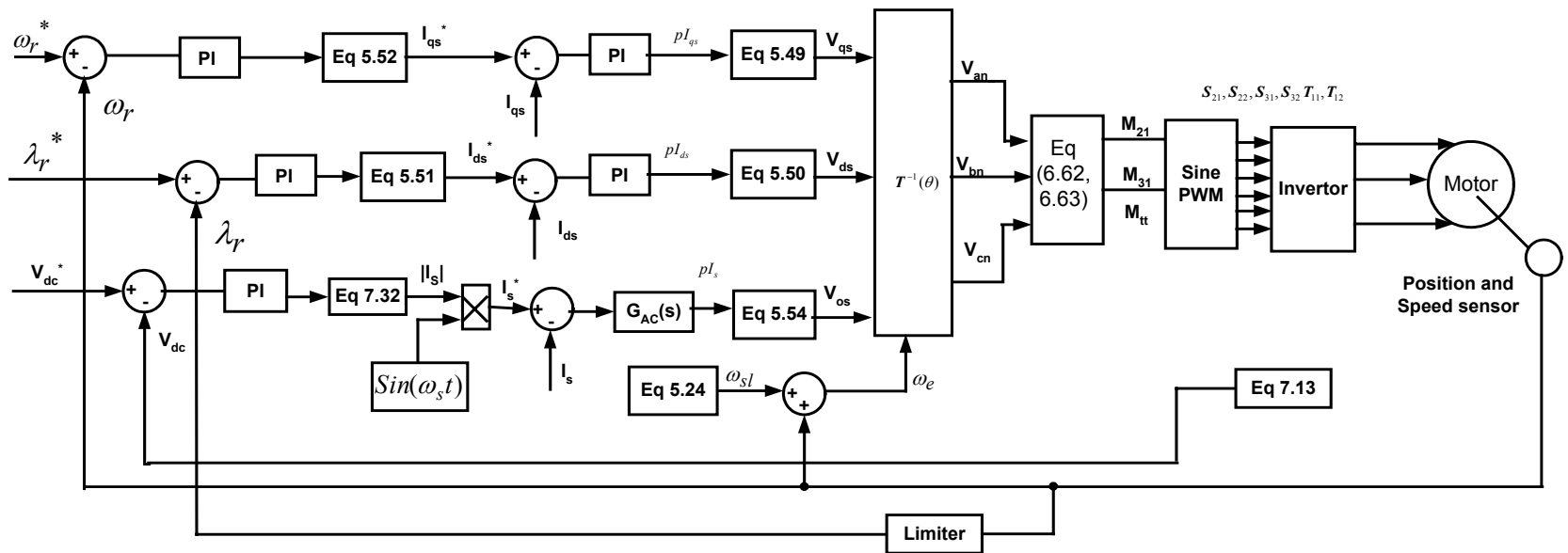
Figure 7.6: Schematic of controller Structure for Converter A.

The speed for the simulation purpose was ramped up from a zero to the rated motor speed that is around 207 rad/sec for operation below the supply frequency. For operation above the supply frequency the speed was ramped up from zero to 400 rad/sec; the single-phase supply voltage is 120V at 60 Hz. Figures 7.7 to 7.12 show the simulation results obtained for Converter A for operation below the supply the supply frequency and 7.13 to 7.18 show the simulation results obtained for operation above the supply frequency. Initially the motor was running on no-load and at 1s a load of 4N-m was added on the machine and the system was allowed to settle to a steady state and then the load was removed at 3s.

Figure 7.7 (a) and 7.13(a) show the dc voltage regulated to 500 V and 800 V respectively, it can be seen that the voltage reduces slightly when the load is added but it gradually builds up to be constant, 7.7(b) and 7.13(b) show the supply voltage and current, which are almost in phase with each other. The supply voltage is scaled by some factor so that both the voltage and current can be seen clearly. It can be seen that the supply current is not very much balanced due to the fact that the three phases are not symmetric.

Figure 7.8(a), 7.8(b) 7.14(a) and 7.14 (b) all show the motor frequency and the rotor speed, following any change it can be seen that to keep the rotor speed constant the motor frequency is slightly increased. Figures 7.8(c),(d) and 7.14 (c) and (d) show the slip speed and the electromagnetic torque when a load torque of 4 N-m is added on to the machine.

In Figure 7.9 and 7.15 show the rotor flux is shown which follows the command. Figure 7.10(a) and 7.16(a) shows the three-phase load currents after the removal of the component $I_s/3$ are plotted against time when the load on the machine persists. In the (b) part the actual current flowing into the stator is plotted. Figures 7.12 and 7.17 show the unfiltered and the filtered phase voltages. It can be seen that the phase 'a' voltage does not contain any switching as it is directly connected to the capacitor leg. Figure 7.13 shows the modulation signals for the three legs.
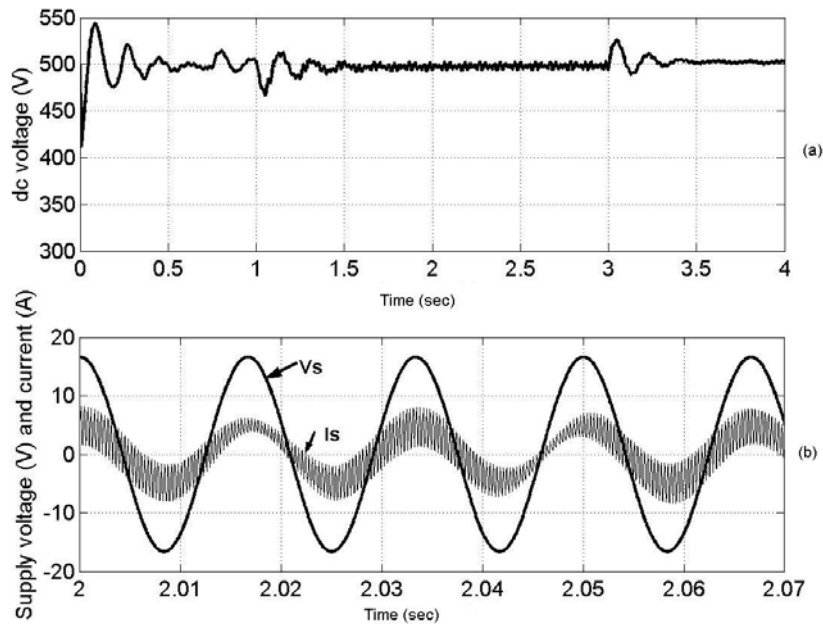
Figure 7.7: Regulated dc voltage, $\omega_r^* = 207\,rad/\sec$ (a) the dc link voltage for a load change of 4 N-m, (b) The supply voltage and the supply current for the same load change.
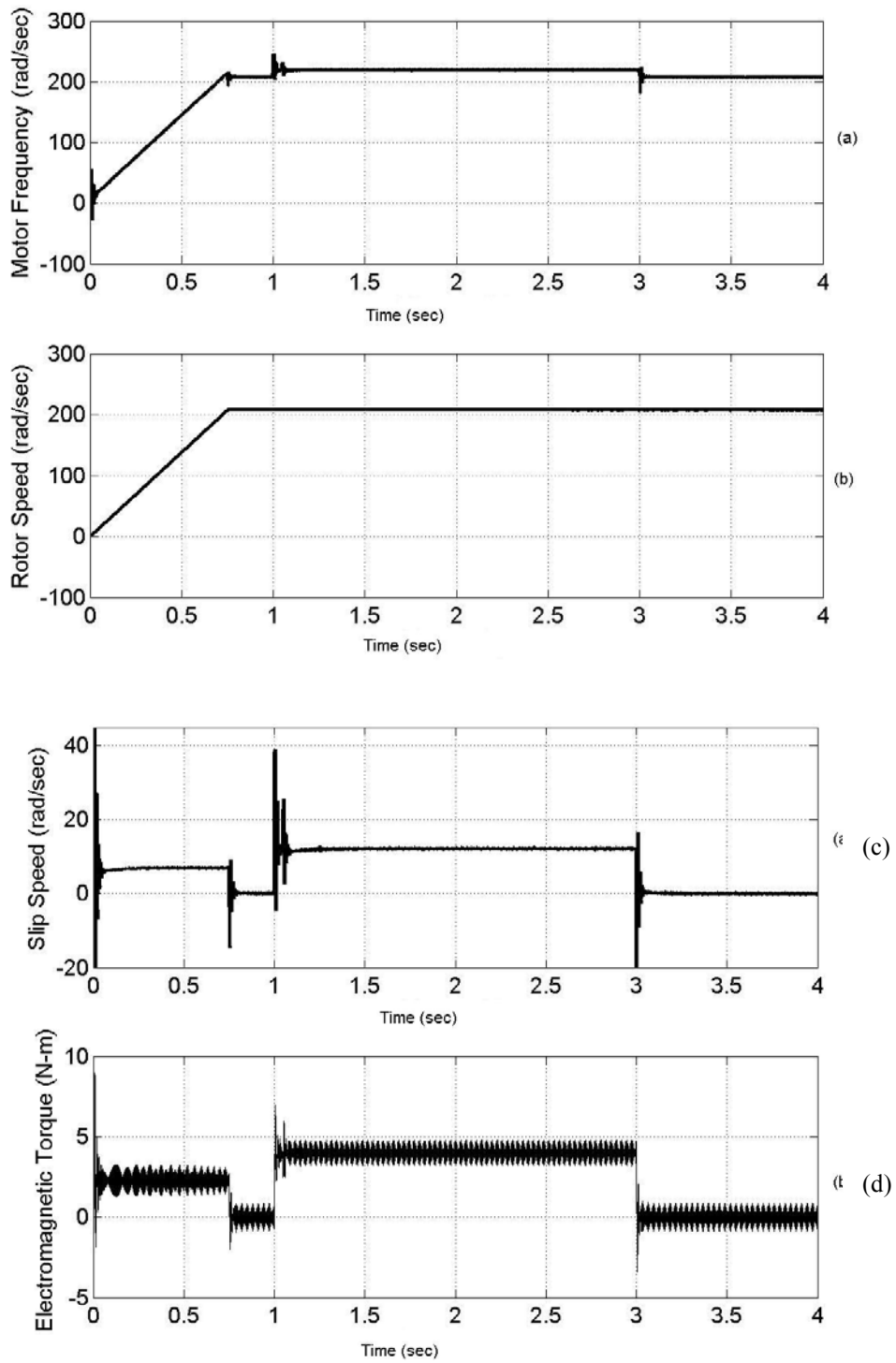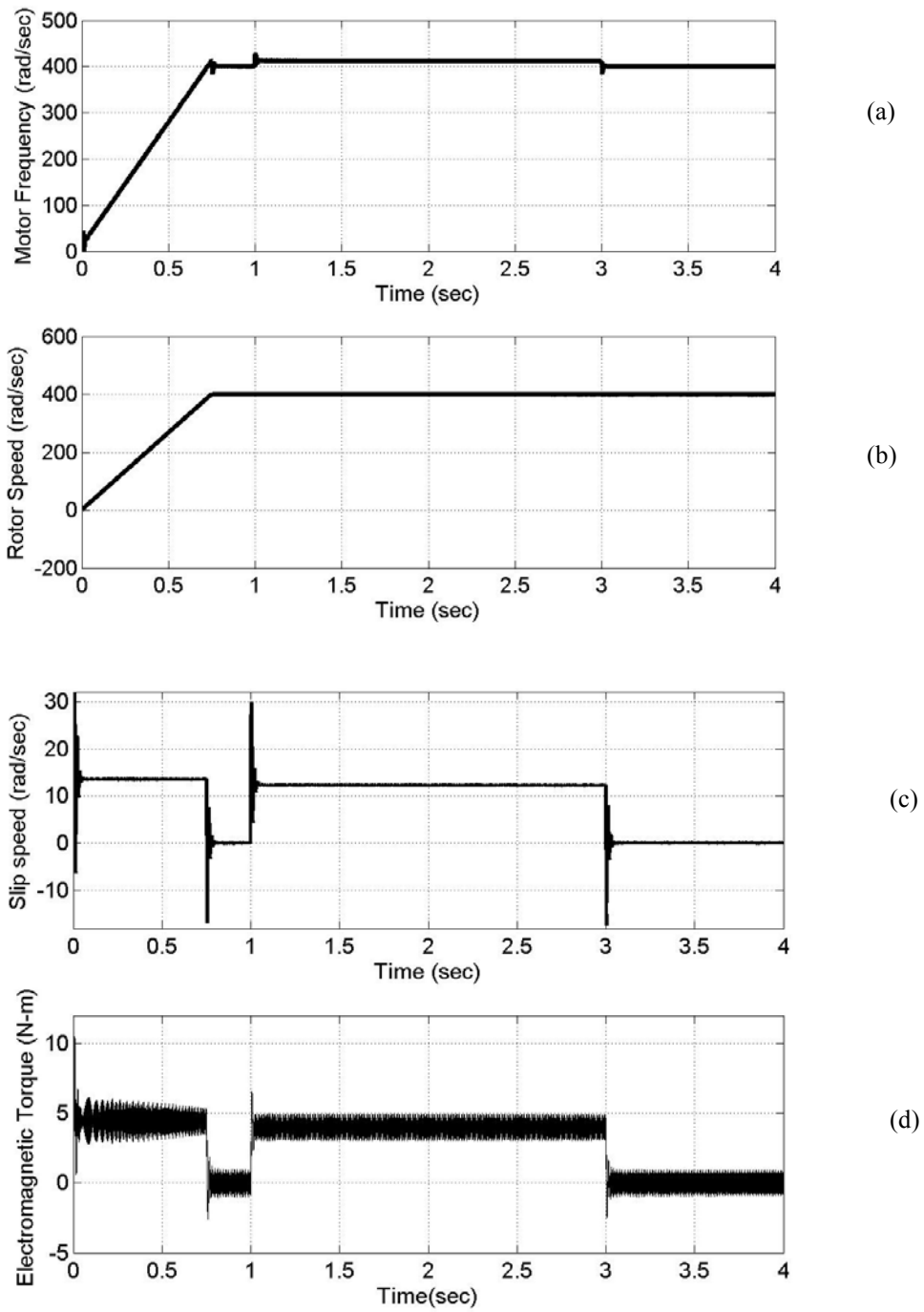
Figure 7.8: Load change, $\omega_r^* = 207\,rad/\sec$. (a) motor frequency in rad/sec, (b) the rotor speed and the command in rad/sec, (c) the slip speed (d) the electromagnetic torque of 4 N-m
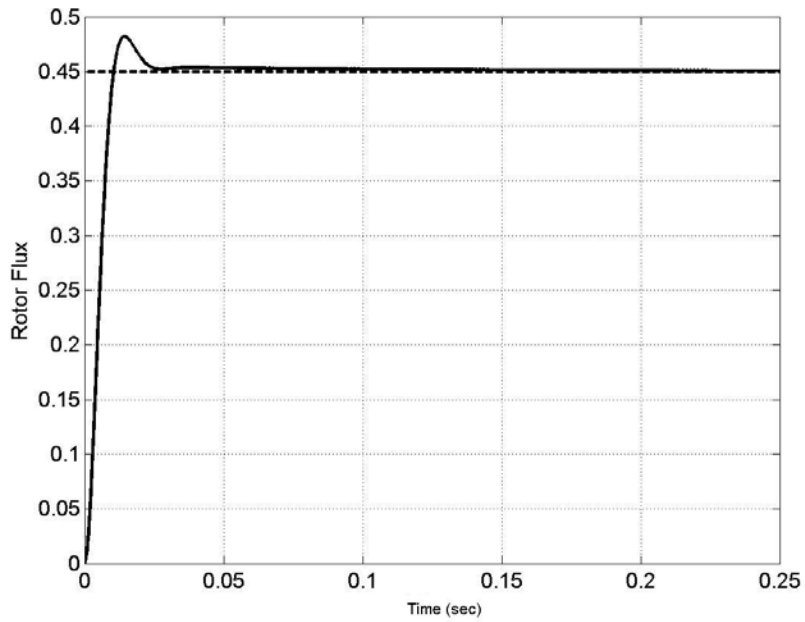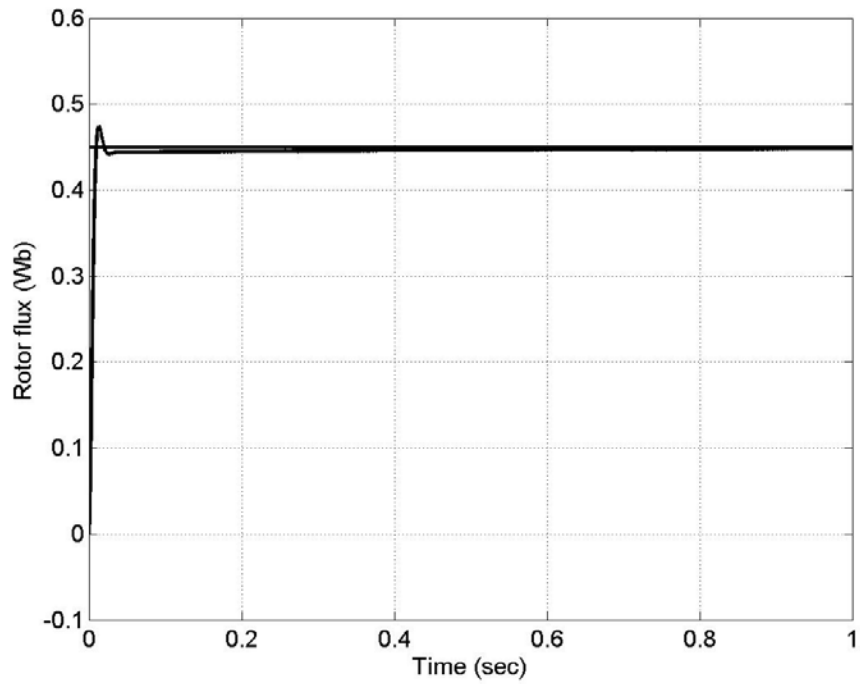
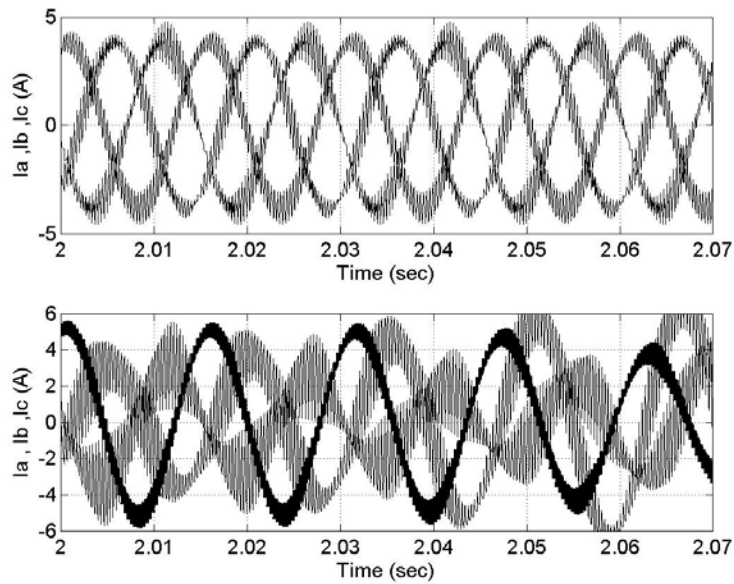Figure 7.9: Rotor flux in Webers, $\omega_r^* = 207\,rad/\sec$.
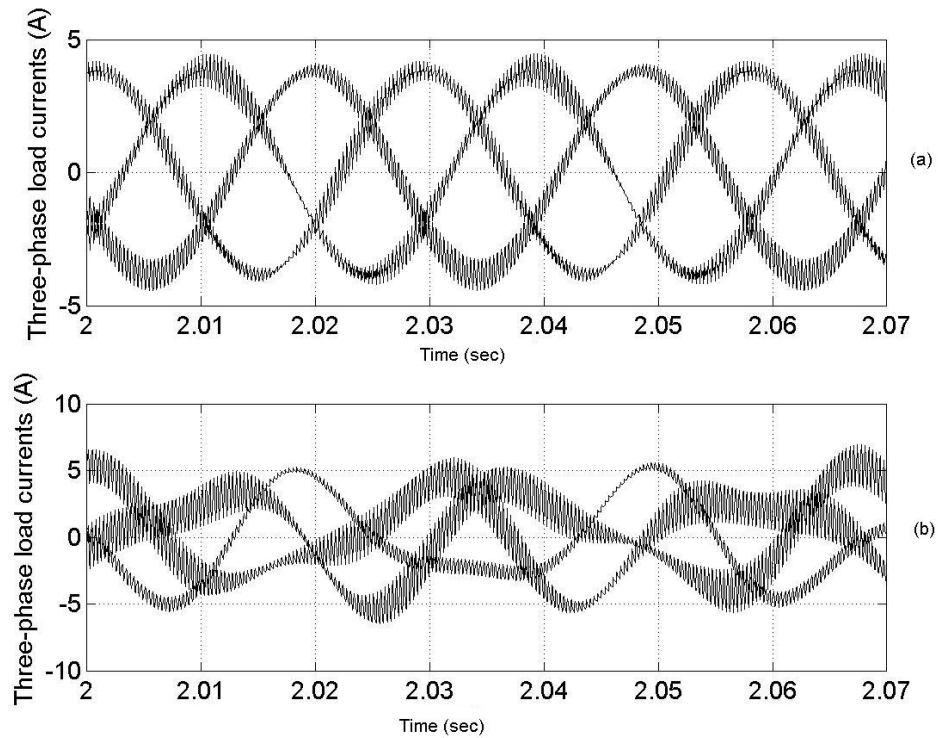
Figure 7.10: On load of 4 N-m, $\omega_r^* = 207\,rad/\sec$ (a) load currents after removal of supply current, (b) the actual load currents
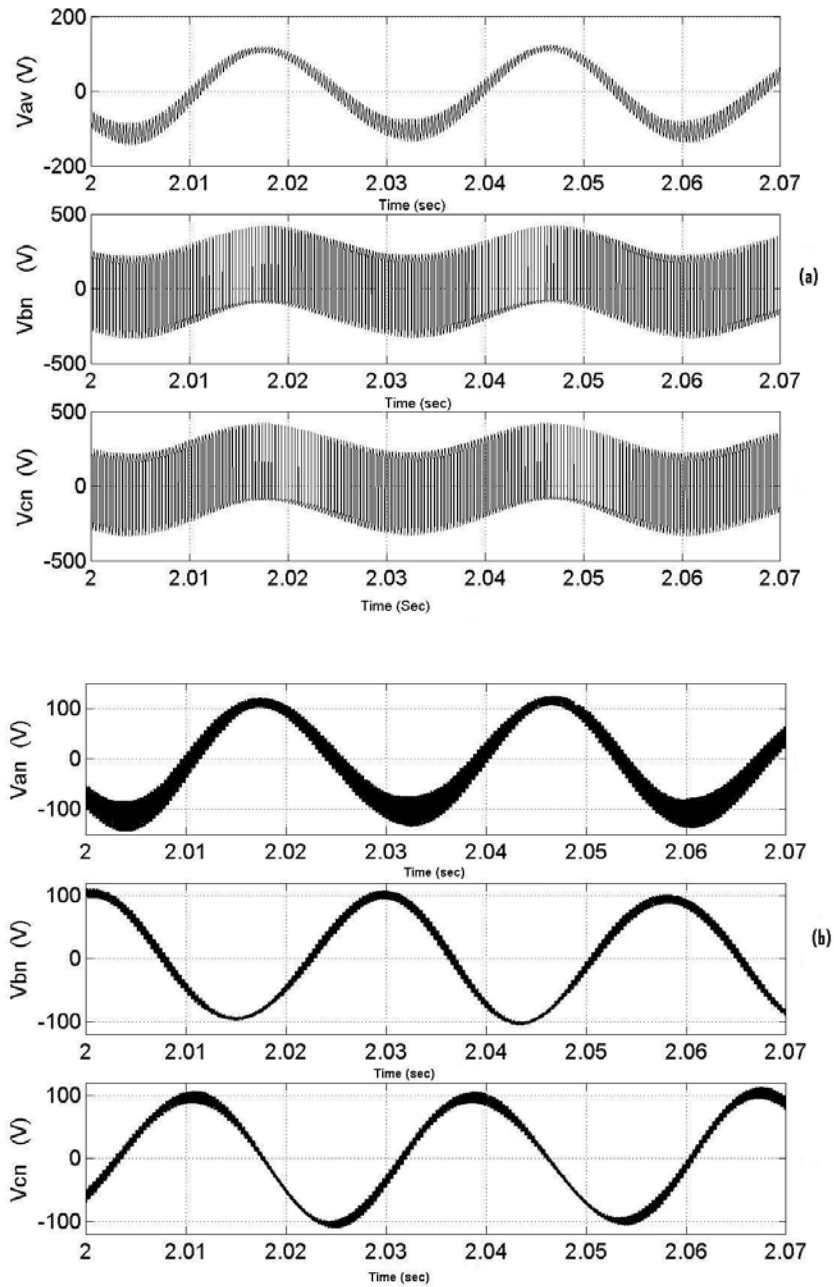
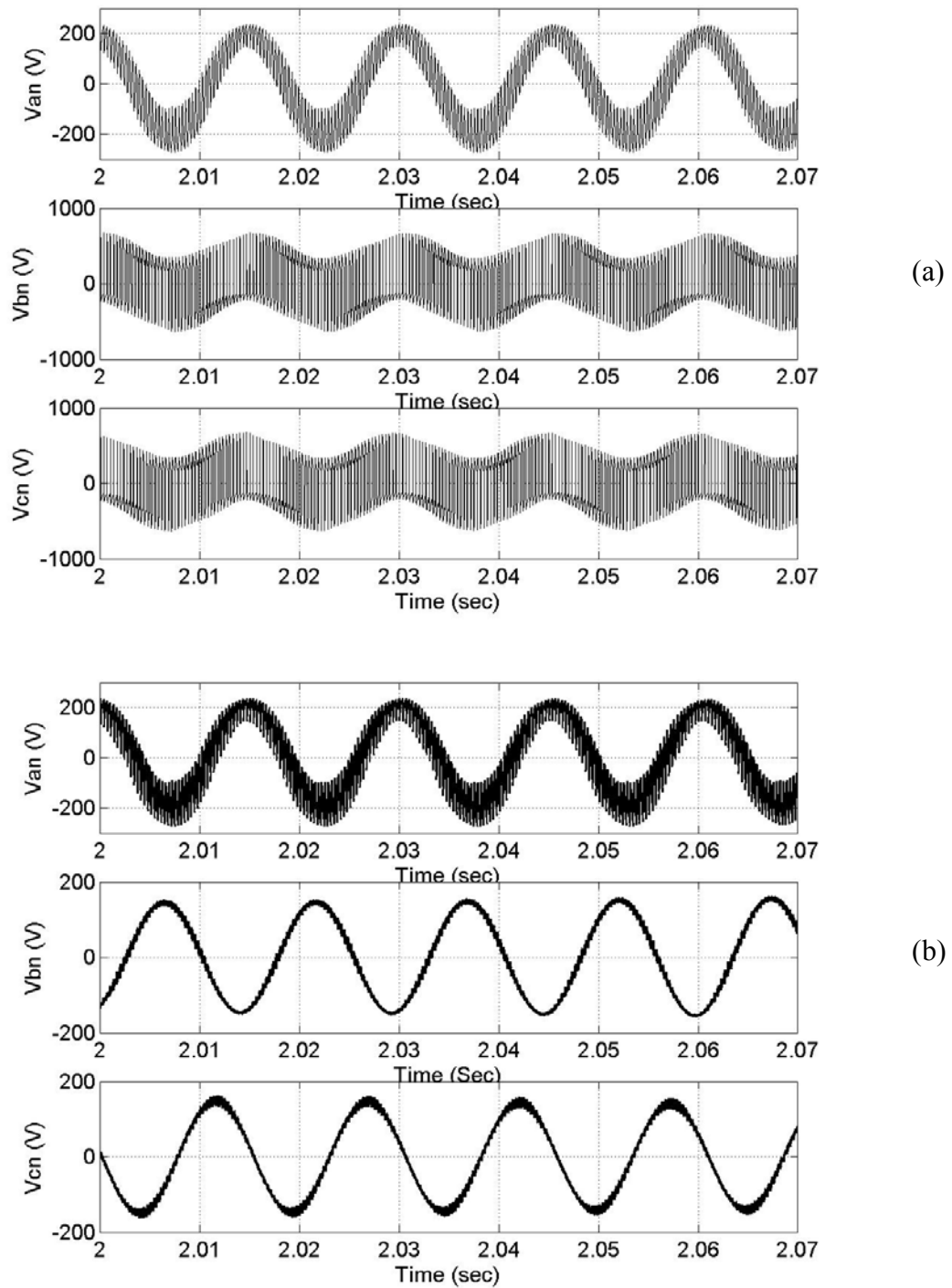Figure 7.11: On load of 4 N- m, $\omega_r^* = 207\,rad/\sec$ (a) the three-phase unfiltered load voltages (V_{an}, V_{bn}, V_{cn}), (b) the three-phase load voltages after filtering the harmonic components.
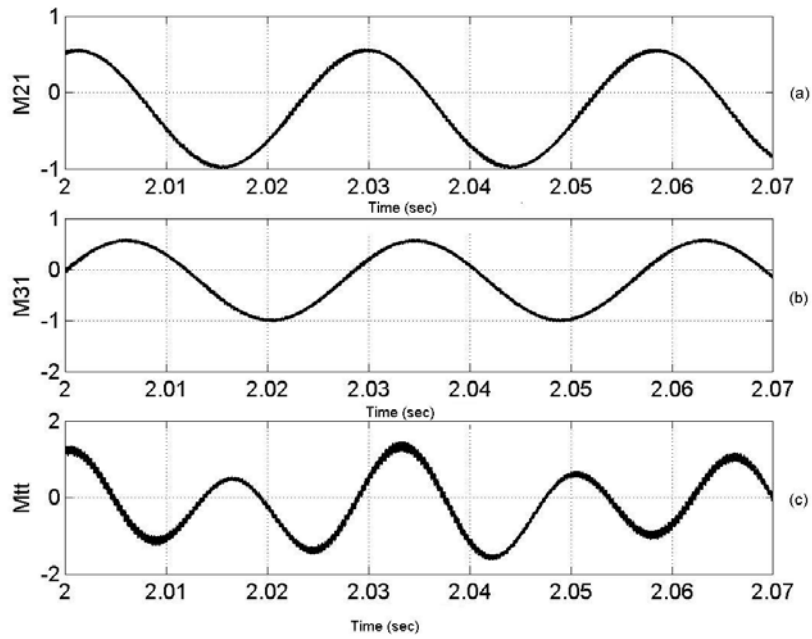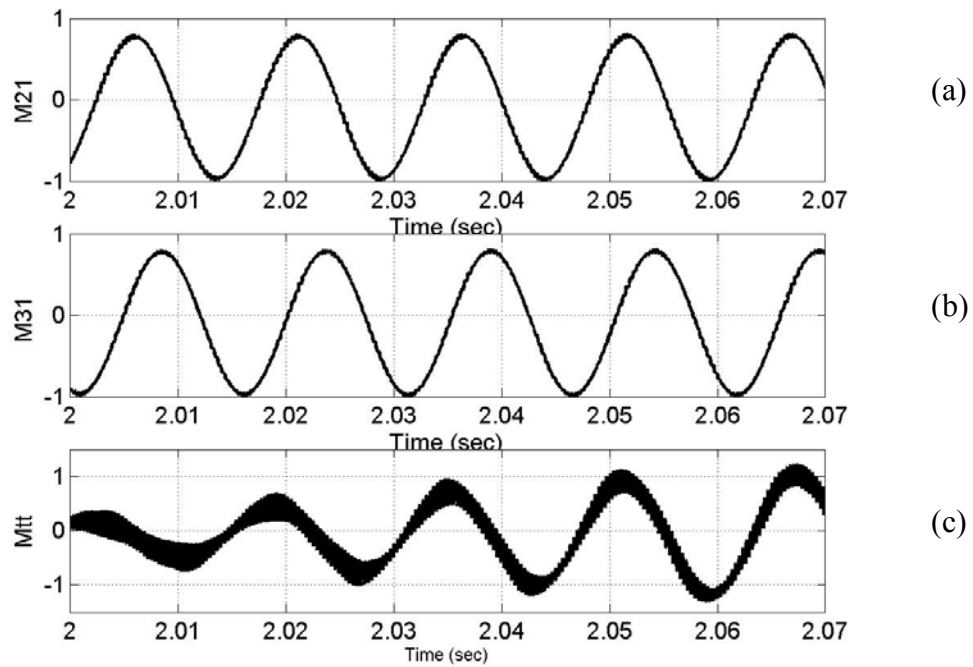
Figure 7.12: Modulation signals, $\omega_r^* = 207\,rad/\sec$ (a) M_{11} (b) M_{21} (c) M_{tt}. Simulation results for operation above supply frequency:
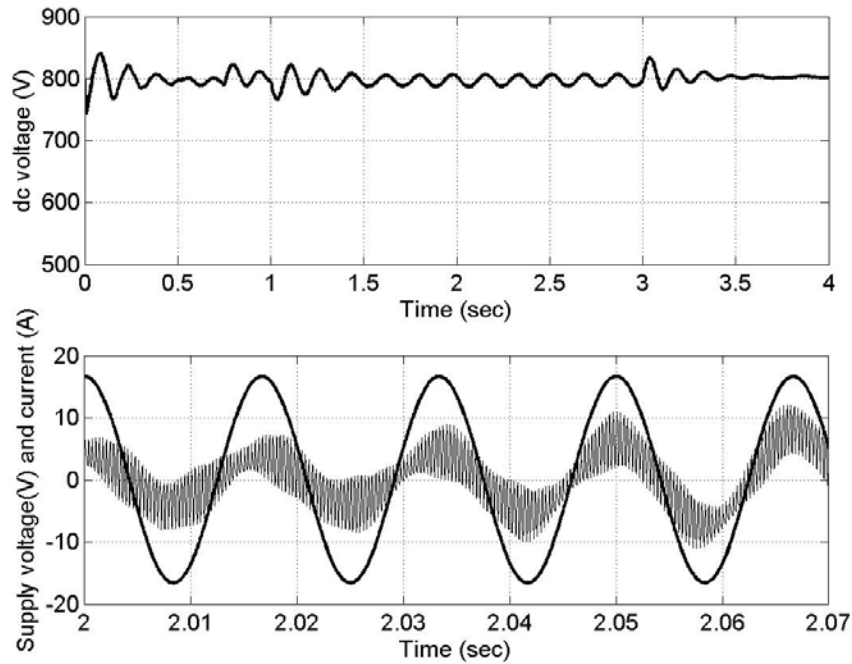
Figure 7.13: Regulated dc voltage, $\omega_r^* = 400\,rad/\sec$ (a) the dc link voltage for a load change of 4 N-m, (b) The supply voltage and the supply current for the same load change.

Figure 7.14: Load change, $\omega_r^* = 400 \ rad / \sec$. (a) motor frequency in rad/sec, (b) the rotor speed and the command in rad/sec, (c) the slip speed (d) the electromagnetic torque of 4 N-m

153

Figure 7.15: Rotor flux in Webers , $\omega_r^* = 400 \; rad/\sec$.

Figure 7.16: On load of 4 N-m, $\omega_r^* = 400 \; rad/\sec$ (a) load currents after removal of supply current, (b) the actual load currents

154

Figure 7.17: On load of 4 N- m, $\omega_r^* = 400\ rad\,/\sec$ (a) the three-phase unfiltered load voltages (V_{an}, V_{bn}, V_{cn}), (b) the three-phase load voltages after filtering the harmonic components.

Figure 7.18: Modulation signals, $\omega_r^* = 400 \ rad/\sec$ (a) M_{11} (b) M_{21} (c) M_{tt}.

7.4 Converter B

The model for the converter B is as shown in Fig 7.19. This circuit is a modification of the conventional half-bridge ac-to-dc converter. The capacitive leg with accessible neutral point corresponds to the converter. The circuit is very simple as it uses only six switching devices however the dc link capacitor voltage is more when compared to the contemporary full bridge converter which imposes the condition that the switches should be able to withstand higher voltage.
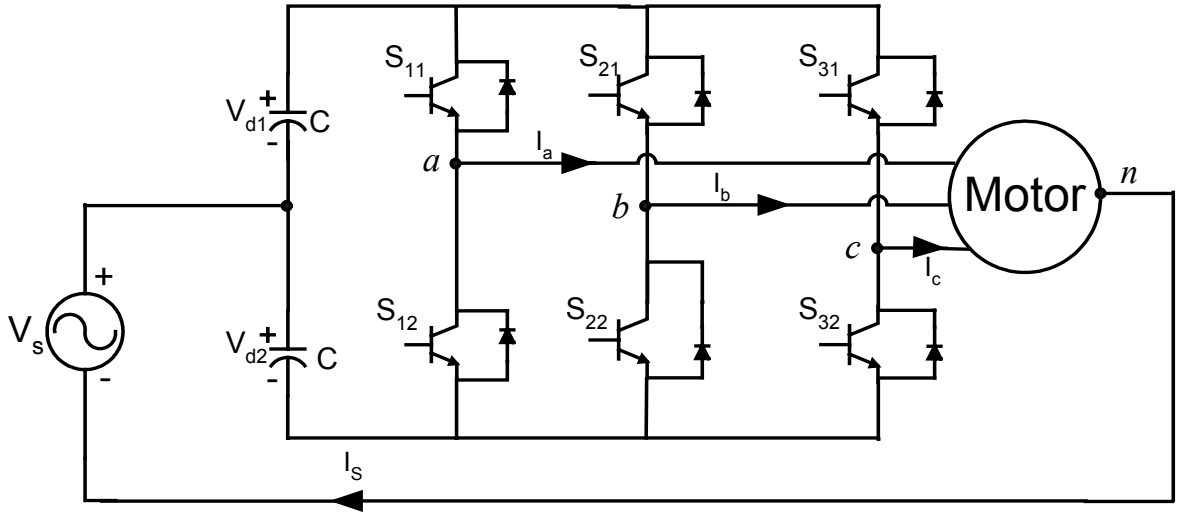
Figure 7.19: Circuit Model for Converter B

Analyzing Figure 7.16 the expressions for the modulating signals of the switching devices. The equations, which describe the circuit, are

$$V_{d1}S_{11} - V_{d2}S_{12} = V_{an} - V_s \tag{7.33}$$

$$V_{d1}S_{21} - V_{d2}S_{22} = V_{bn} - V_s \tag{7.34}$$

$$V_{d1}S_{31} - V_{d2}S_{32} = V_{cn} - V_s \tag{7.35}$$

The behavior of the switching devices in each leg is complimentary and so the following constraints can be written

$$S_{11} + S_{21} = 1$$

$$S_{21} + S_{22} = 1 \tag{7.36}$$

$$S_{31} + S_{32} = 1$$

Using KCL

$$CpV_{d1} = -(I_a T_{11} + I_b T_{21} + I_c T_{31}) \tag{7.37}$$

157

$$CpV_{d2} = (I_aT_{21} + I_bT_{22} + I_cT_{32})$$ (7.38)

where $V_{d1} + V_{d2} = V_d$ (the dc link voltage) and $V_{d1} - V_{d2} = V_\sigma$ (the ripple that can be accepted)

$$CpV_d = -(I_a(2S_{11} - 1) + I_b(2S_{21} - 1) + I_c(2S_{31} - 1))$$ (7.39)

$$CpV_\sigma = -(I_a + I_b + I_c)$$ (7.40)

The switching functions expressed in terms of the modulating signals as

$$S_{11} = \frac{1}{2}(1 + M_{11})$$

$$S_{21} = \frac{1}{2}(1 + M_{21})$$ (7.41)

$$S_{31} = \frac{1}{2}(1 + M_{31})$$

From Equation 7.41 the modulating signals for the control of the switches can be written as

$$M_{11} = \frac{1}{V_d}(2V_{an} - 2V_s - V_\sigma)$$ (7.42)

$$M_{21} = \frac{1}{V_d}(2V_{bn} - 2V_s - V_\sigma)$$ (7.43)

$$M_{31} = \frac{1}{V_d}(2V_{cn} - 2V_s - V_\sigma).$$ (7.44)

M_{11}, M_{21} and M_{31} given in Equations 7.42, 7.43 and 7.44 correspond to the modulation signals for the inverter legs which are used to obtain the pulse widths for the time the respective switches are either on and off.

Equations 7.42 to 7.44 can be written in matrix form as

$$\frac{V_d}{2}\begin{bmatrix} M_{11} \\ M_{21} \\ M_{31} \end{bmatrix} = \begin{bmatrix} V_{an} \\ V_{bn} \\ V_{cn} \end{bmatrix} - \begin{bmatrix} V_s \\ V_s \\ V_s \end{bmatrix} - \begin{bmatrix} V_\sigma/2 \\ V_\sigma/2 \\ V_\sigma/2 \end{bmatrix} \qquad (7.45)$$

Transforming the above matrix into synchronous reference frame (that is the speed with which the motor rotates)

$$\frac{V_d}{2}\begin{bmatrix} m_{qs} \\ m_{ds} \\ m_{os} \end{bmatrix} = \begin{bmatrix} V_{qs} \\ V_{ds} \\ V_{os} \end{bmatrix} - \begin{bmatrix} 0 \\ 0 \\ V_s \end{bmatrix} - \begin{bmatrix} 0 \\ 0 \\ V_\sigma/2 \end{bmatrix} \qquad (7.46)$$

$$m_{qs} = \frac{2V_{qs}}{V_d} \qquad (7.47)$$

$$m_{ds} = \frac{2V_{ds}}{V_d} \qquad (7.48)$$

$$m_{os} = \frac{(2V_{os} - 2V_s - V_\sigma)}{V_d} \qquad . \qquad (7.49)$$

The dc –link current equation can be written as the sum of each of the load current and the supply current as,

$$CpV_d = -(i_a(S_{11} - S_{12}) + i_b(S_{21} - S_{21}) + i_c(S_{31} - S_{32})) \qquad (7.50)$$

or equivalently

$$CpV_d = -(i_a M_{11} + i_b M_{21} + i_c M_{31}) \qquad (7.51)$$

applying synchronous transformation to the above equation by making use of the following equalities ,

$$i_{qdo}{}^T = [(K_s)i_{abc}]^T = i_{abc}{}^T K_s{}^T \tag{7.52}$$

$$i_{abc}{}^T = i_{qdo}{}^T (K_s{}^T)^{-1} \tag{7.53}$$

therefore the dc link current can be written as

$$CpV_d = -(i_{abc}{}^T M_{112131}) \tag{7.54}$$

where $\quad i_{abc}{}^T = [i_a \; i_b \; i_c]^T \quad$ and $\quad M_{112131} = \begin{bmatrix} M_{11} \\ M_{21} \\ M_{31} \end{bmatrix}$

applying 'qdo' transformation for Equation 6.26,

$$CpV_d = -(i_{qdo}{}^T (K_s{}^T)^{-1}(K_s)^{-1} m_{qdo}) \tag{7.55}$$

where $\quad m_{qdo} = [m_{qs} \; m_{ds} \; m_{os}] \quad$ and $\quad (K_s{}^T)^{-1}(K_s)^{-1} = \begin{bmatrix} \dfrac{3}{2} & 0 & 0 \\ 0 & \dfrac{3}{2} & 0 \\ 0 & 0 & 3 \end{bmatrix}$, and so equation

6.27 can be written as

$$CpV_d = -(1.5m_{qs}i_{qs} + 1.5m_{ds}i_{ds} + 3m_{os}i_{os}) \tag{7.56}$$

as $i_{os} = \dfrac{i_s}{3}$ Equation 7.56 can be written as

$$CpV_d = -(1.5m_{qs}i_{qs} + 1.5m_{ds}i_{ds} + m_{os}i_s) \tag{7.57}$$

or

$$i_s = CpV_d + 1.5m_{qs}i_{qs} + 1.5m_{ds}i_{ds} \ .$$ (7.58)

where i_s the fundamental component of the supply current.

7.4.1 Control Scheme for Converter B

The control objective for this Converter on the line side is to regulate supply current to be in phase with the voltage, and to maintain the dc voltage at a constant value, on the load side speed and flux control are done owing to any change in the load on the machine. The control structure can be explained as, regulation of speed gives the reference command for the q-axis stator current and the regulation of rotor flux gives the reference command for the d-axis stator current. The q-axis and the d-axis currents are compared with the calculated values and the error is processed through a PI controller and using the feedback linearization control technique as explained in the previous chapters, followed by some calculations the reference q and d-axis stator voltages (v_{qs}, v_{ds}) are obtained. When they are normalized by the dc voltage the q and d-axis values (m_{qs} and m_{ds}) of the modulation signals are obtained.

The dc voltage is regulated and the output is used to get the reference magnitude for the supply current, this supply current can be filtered to obtain a pure dc signal, this dc signal is multiplied with the instantaneous phase angle of the supply voltage this serves as a reference for the supply current.

The three phase currents by virtue of the circuit connection contain on-third component of the supply current and so by sensing the three-phase currents and summing them together gives the supply current this current is compared with the reference supply current and the output is used to calculate the zero-sequence voltage v_{os}. The zero sequence voltage is normalized to get m_{os}. The values of m_{qs}, m_{ds} and m_{os} are converted to abc co-ordinates using the frequency calculated by adding the slip speed and the rotor speed. The modulation signals obtained after the transformation are M_{11}, M_{21}, and M_{31} which are compared with a high frequency carrier, to obtain the switching pulses for the switching devices and the voltages obtained are applied to the motor.

The modulation signals M_{11}, M_{21}, and M_{31}, which are the reference commands, are the outputs of the controller, reflect those values which when applied to the controller give the desired response for the system. The overall control structure for the Converter B is as given in Figure 7.20.

7.4.2. Simulation Results

The Converter B as shown in Figure 7.19 was simulated using Induction machine similar to the one used for the simulation of the conventional converters. The simulation results include the various quantities of interest like the speed, dc voltage, supply voltage, currents etc.,
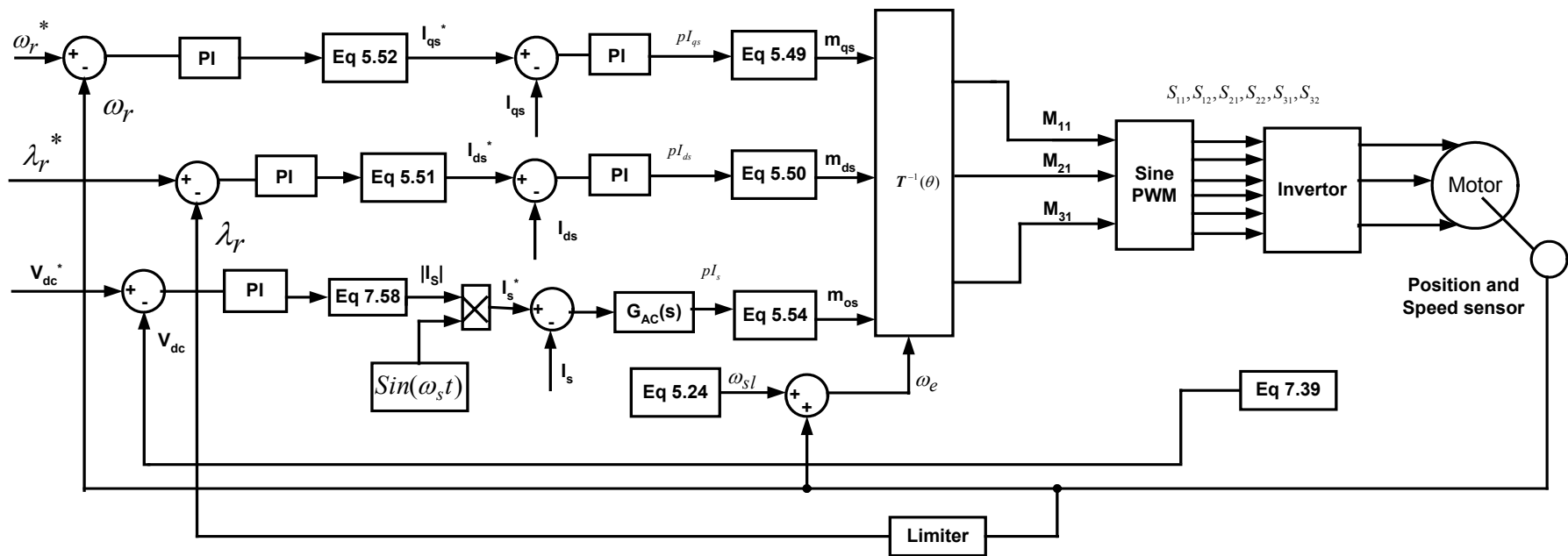
Figure 7.20: Schematic of controller Structure for Converter B.

The speed in this case was ramped up from a zero to the rated motor speed that is around 207 rad/sec. For operation above the supply frequency the speed was ramped up from zero to 400 rad/sec; the single-phase supply voltage is 120V at 60 Hz. Figures 7.21 to 7.26 show the simulation results obtained for Converter A for operation below the supply the supply frequency and 7.27 to 7.32 show the simulation results obtained for operation above the supply frequency. Initially the motor was running on no-load and at 1s a load of 4N-m was added on the machine and the system was allowed to settle to a steady state and then the load was removed at 3s.

Figures 7.21 (a) and 7.27(a) show the dc voltage, it can be seen that the voltage reduces slightly when the load is added but it gradually builds up to be constant at its rated value, figures 7.21(b) and 7.27(b) show the supply voltage and current, which are almost in phase with each other. The supply voltage is scaled by some factor so that both the voltage and current can be seen clearly. It can be seen that the dc voltage for this converter is very high when compared to the other topologies due to the fact that the capacitor is the only charging element and supplies voltage to the load. The supply current is not very much balanced due to the fact that the three phases are not symmetric.

Figures 7.22(a), 7.22(b), 7.28(a) and 7.28(b) show the motor frequency and the rotor speed, following any change it can be seen that to keep the rotor speed constant the motor frequency is slightly increased. In Figure 7.22 (c), (d) and 7.28

(c),(d) the slip speed and the electromagnetic torque when a load torque of 4 N-m is added on to the machine is shown.

In Figures 7.23 and 7.29 the rotor flux is shown which follows the command. Figures 7.24 (a) and 7.30(a) show the three-phase actual load currents and Figures 7.24(b) and 7.30 (b) show the plot of load currents after the removal of the component $I_s/3$ versus time.

Figures 7.25 and 7.31show the unfiltered and the filtered phase voltages. Finally in Figures 7.26 and 7.32 the modulation signals for the three legs are shown.

(a)

(b)
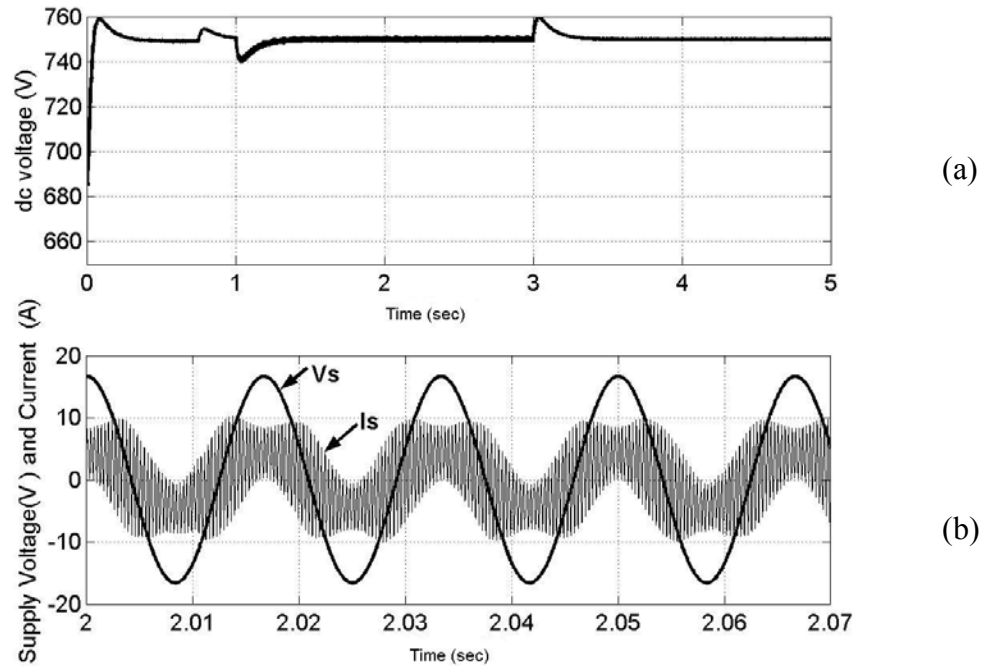
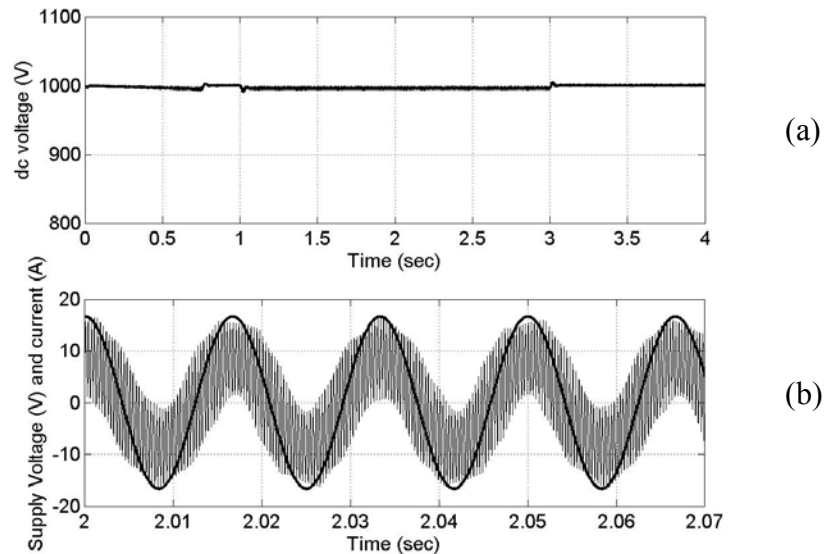Figure 7.21: Regulated dc voltage, $\omega_r^* = 207 \ rad/\sec$ (a) dc voltage regulated at 750V, (b) supply voltage and supply current superimposed on each other.
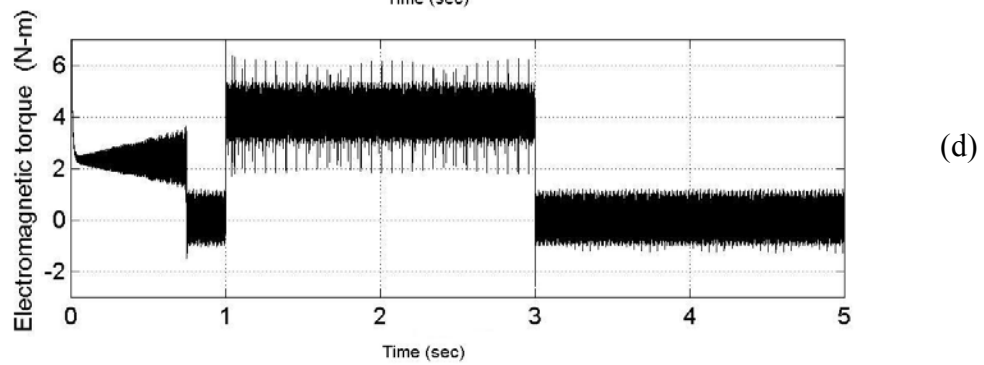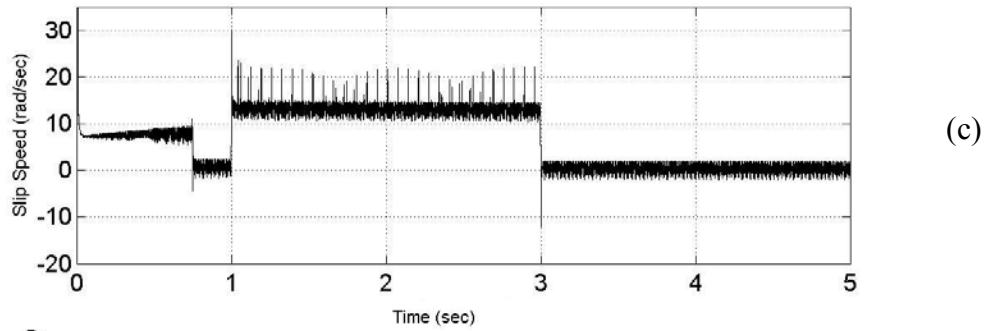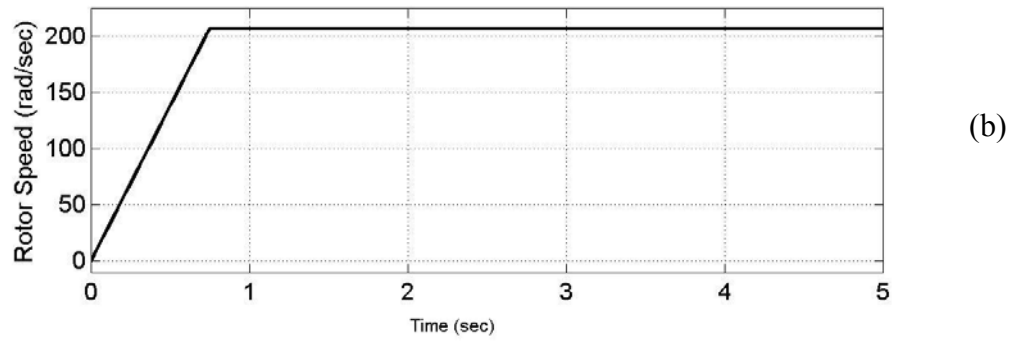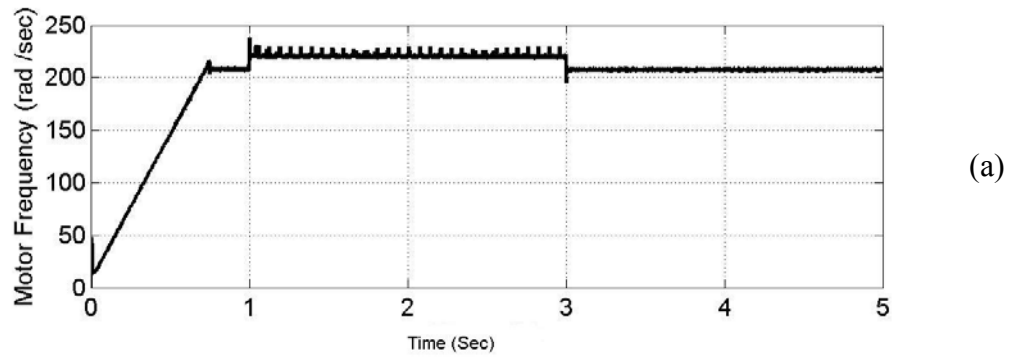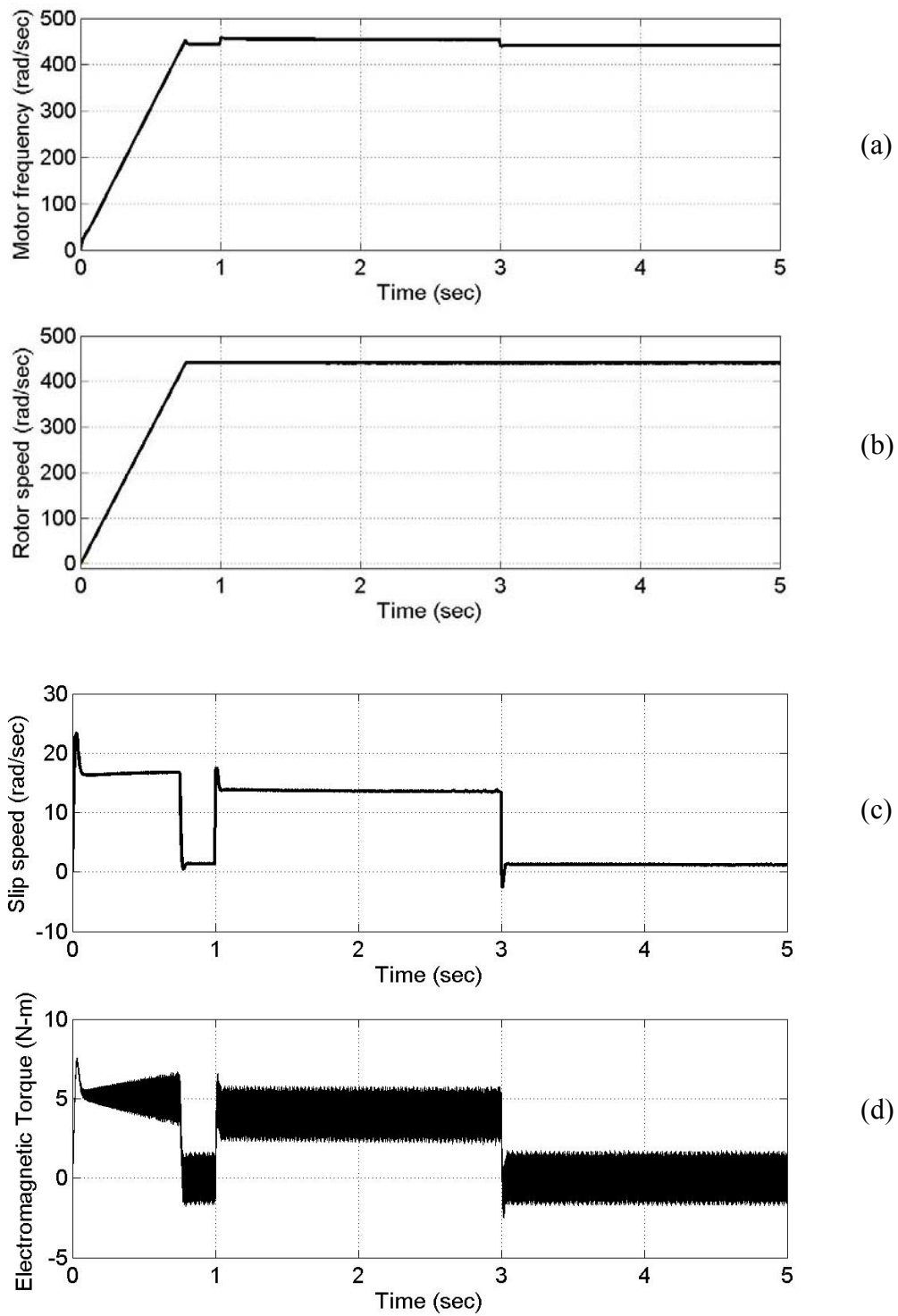
Figure 7.22: Load change, $\omega_r^* = 207\ rad/\sec$ (a) The motor frequency in rad/sec, (b) the rotor speed, (c) the slip speed, (d) the electromagnetic torque of 4 N-m.
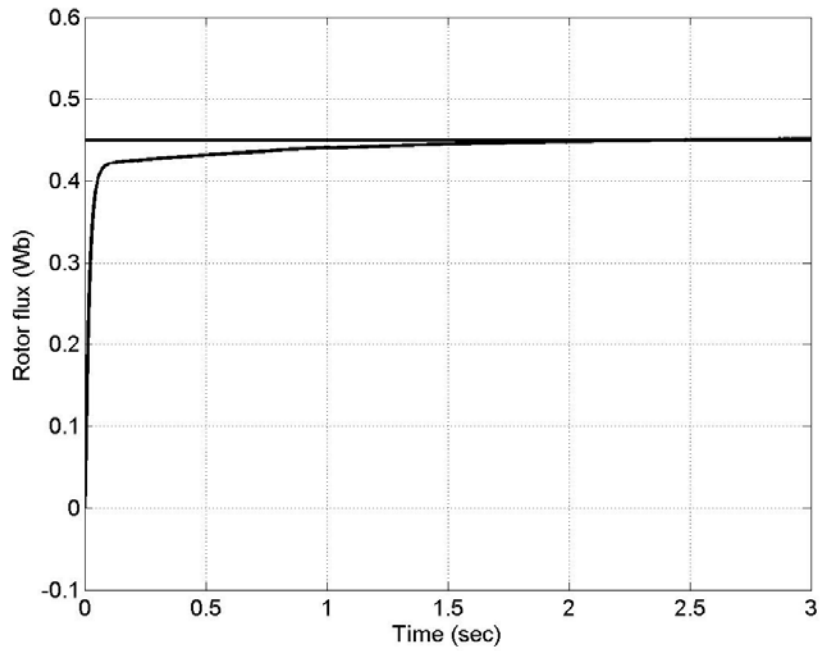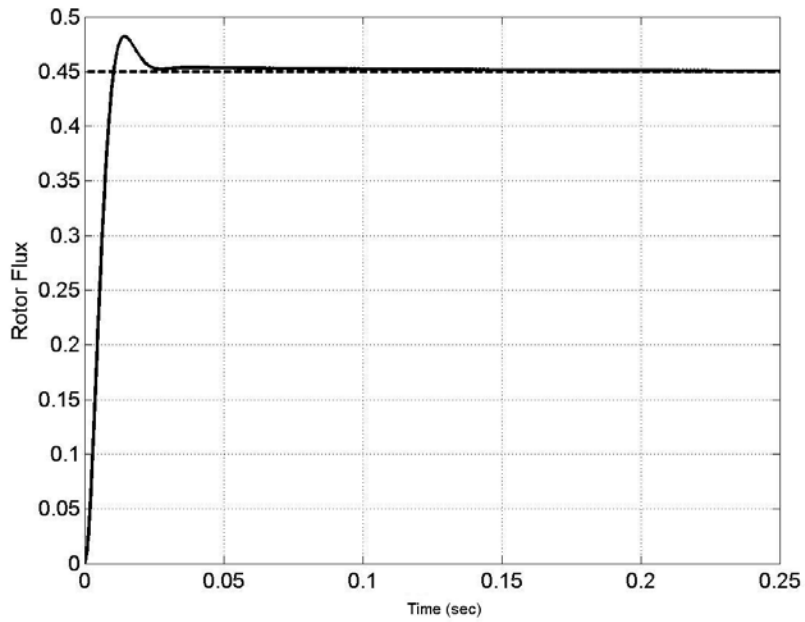
Figure 7.23: Rotor flux in Webers, $\omega_r^* = 207\ rad\,/\sec$.

(a)

(b)
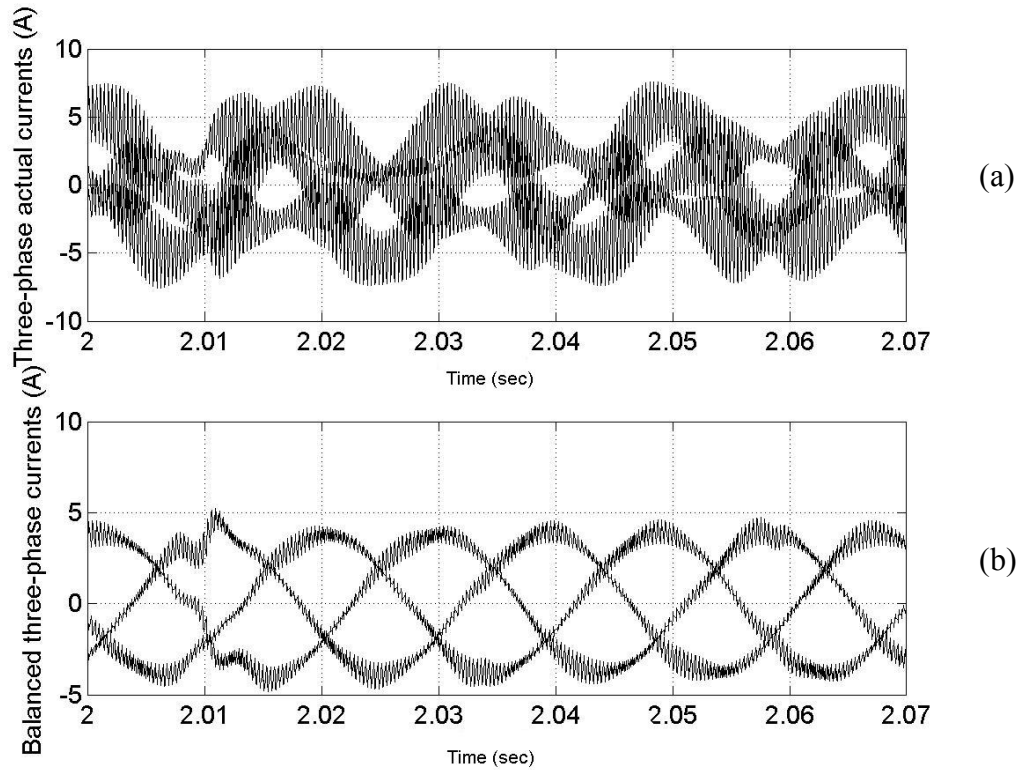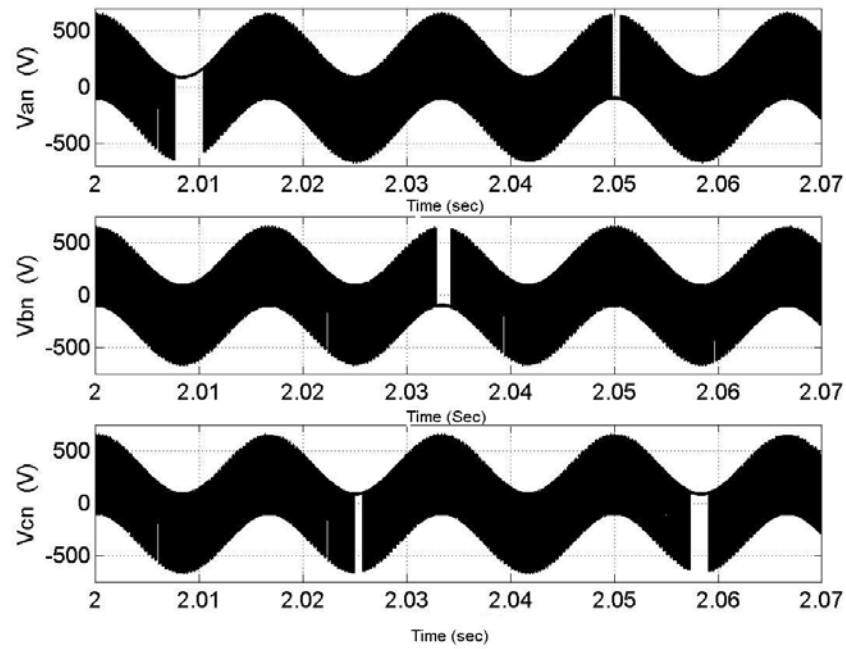
Figure 7.24: On load of 4 N-m, $\omega_r^* = 207\ rad\,/\sec$ (a) load currents after removal of supply current, (b) the actual load currents

167
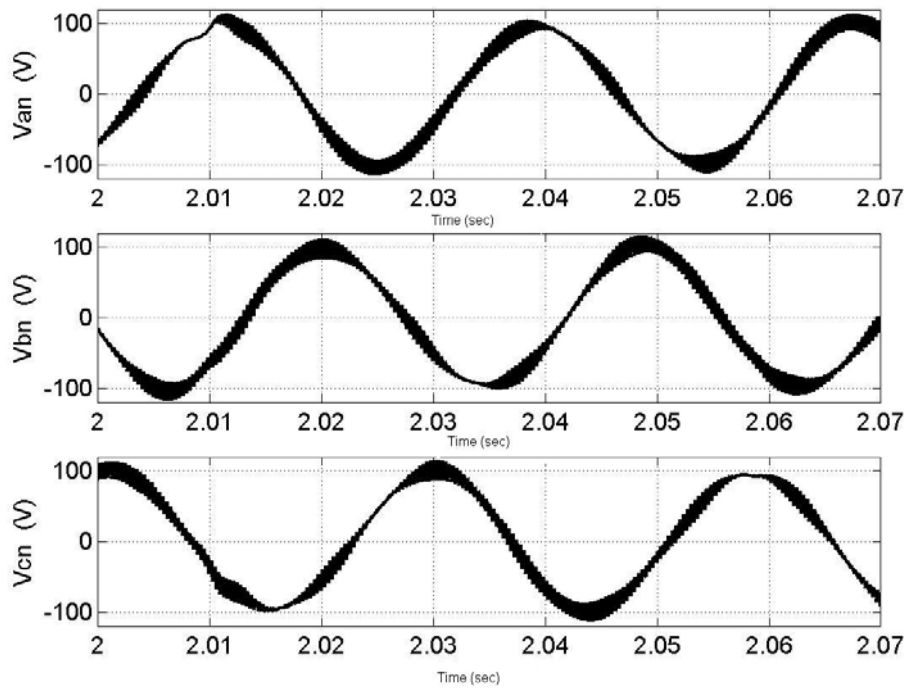
Figure 7.25: On load of 4 N- m, $\omega_r^* = 207\ rad/\sec$ (a) the three-phase unfiltered load voltages (V_{an}, V_{bn}, V_{cn}), (b) the three-phase load voltages after filtering the harmonic components.

Figure 7.26: Modulation signals, $\omega_r^* = 207 \; rad/\sec$ (a) M_{11} (b) M_{21} (c) $M_{tt.}$

Operation above supply frequency:

Figure 7.27: Regulated dc voltage, $\omega_r^* = 400 \; rad/\sec$ (a) dc voltage regulated at 750V, (b) supply voltage and supply current superimposed on each other.

(a)

(b)

(c)

(d)

Figure 7.28: Load change, $\omega_r^* = 400\ rad/\sec$ (a) The motor frequency in rad/sec, (b) the rotor speed, (c) the slip speed, (d) the electromagnetic torque of 4 N-m.

Figure 7.29: Rotor flux in Webers, $\omega_r^* = 400 \ rad/\sec$.

(a)

(b)
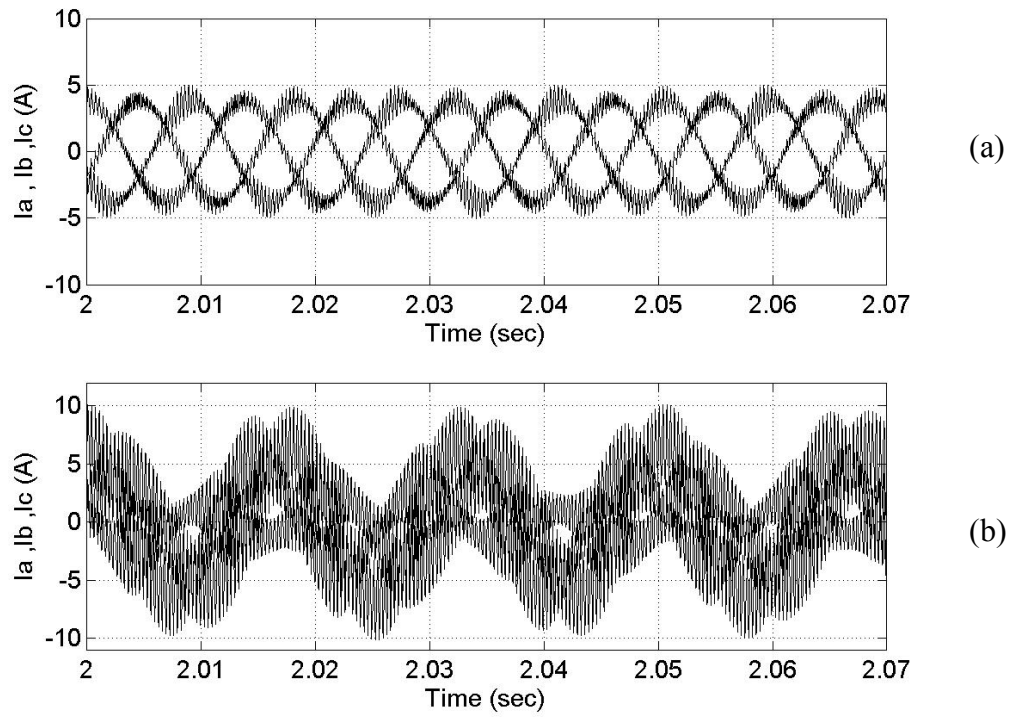
Figure 7.30: On load of 4 N-m , $\omega_r^* = 400 \ rad/\sec$ (a) load currents after removal of supply current, (b) the actual load currents
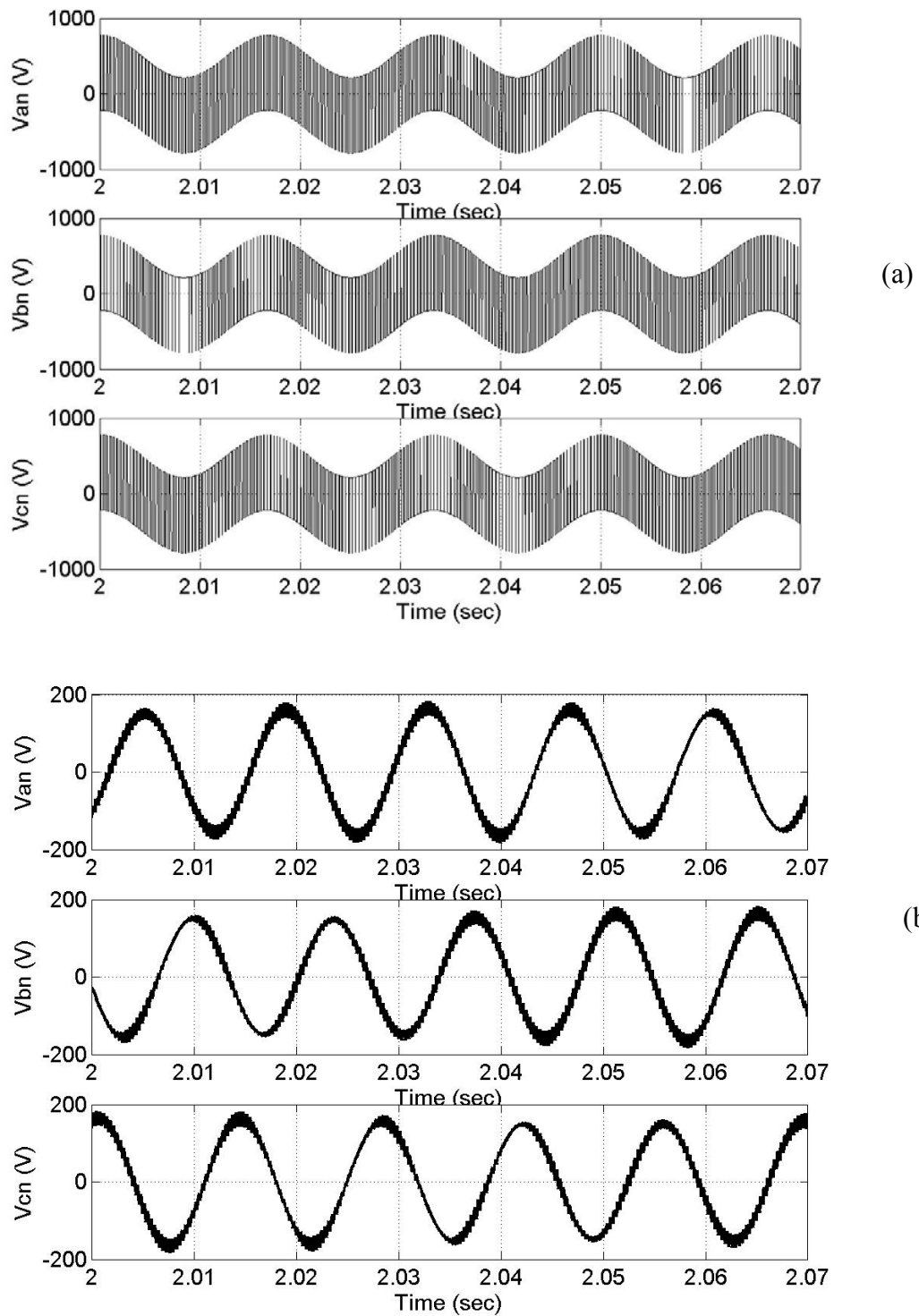
Figure 7.31: On load of 4 N- m, $\omega_r^* = 400$ *rad* / sec (a) the three-phase unfiltered load voltages (V_{an}, V_{bn}, V_{cn}), (b) the three-phase load voltages after filtering the harmonic components.
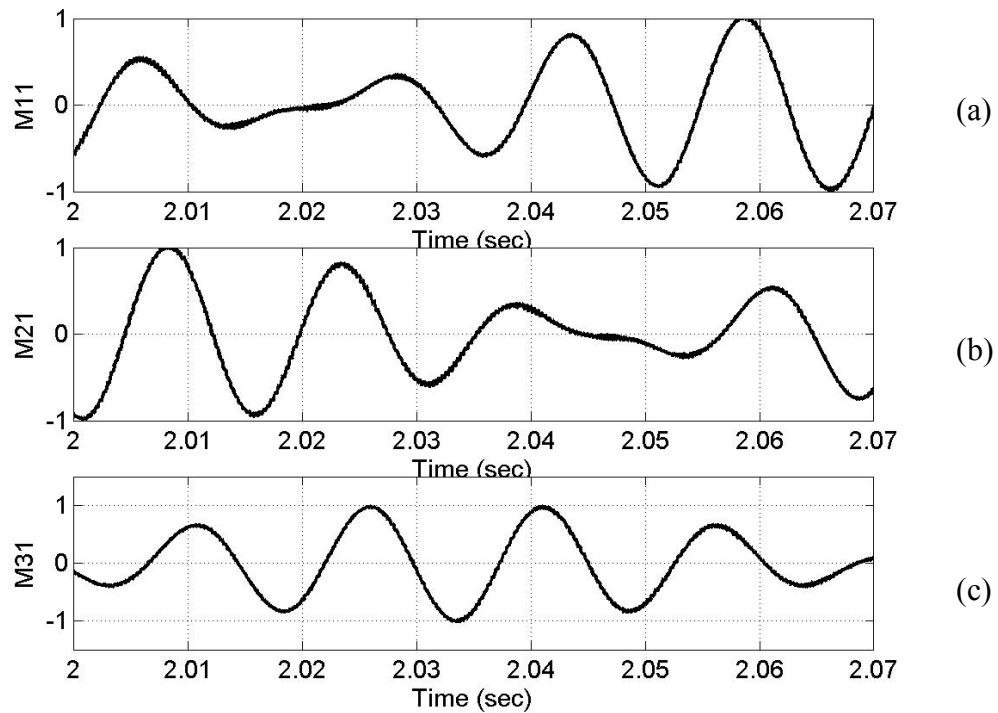
172

Figure 7.32: Modulation signals, $\omega_r^* = 400 \; rad/\sec$ (a) M_{11} (b) M_{21} (c) $M_{tt.}$

7.5 Converter C

The third model of the sparse converters is Converter C shown in Fig 7.33. This circuit is a modification of the conventional full-bridge ac-to-dc converter with four switches. In this converter one of the converter leg is replaced by a capacitor and the power supply is connected to the neutral point of the motor. This circuit requires less dc voltage when compared to the half bridge converter, but it consists of more number of switching devices.
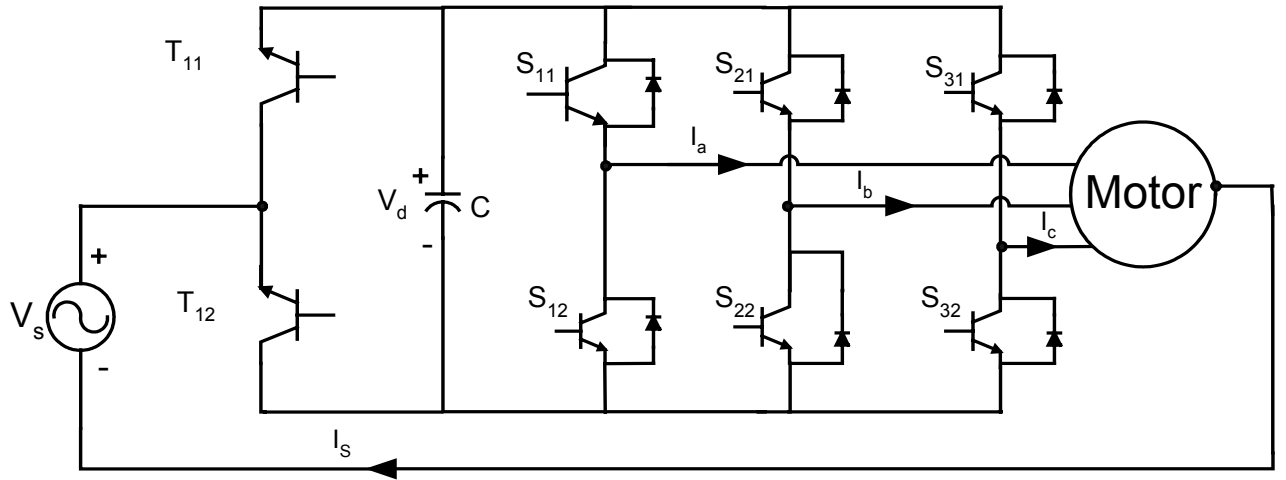
Figure 7.33: Circuit model for converter C

$$\frac{V_d}{2}(S_{11} - S_{12}) = V_{an} + V_{no} \tag{7.59}$$

$$\frac{V_d}{2}(S_{21} - S_{22}) = V_{bn} + V_{no} \tag{7.60}$$

$$\frac{V_d}{2}(S_{31} - S_{32}) = V_{cn} + V_{no} \tag{7.61}$$

In the Equations from 7.59 to 7.61, V_{no} is the voltage at the neutral point of the motor with respect to ground. Since the nature of the switching devices in each leg is complementary the above equations can be written as,

$$\frac{V_d}{2}S_{11} = \frac{V_d}{2} + V_{an} + V_{no} \tag{7.62}$$

$$\frac{V_d}{2}S_{21} = \frac{V_d}{2} + V_{bn} + V_{no} \tag{7.63}$$

$$\frac{V_d}{2} S_{31} = \frac{V_d}{2} + V_{cn} + V_{no} \tag{7.64}$$

The converter side equations are given as

$$V_{no} = (-V_s - \frac{V_d}{2})T_{12} + T_{11}(-V_s + \frac{V_d}{2}) \tag{7.65}$$

or $V_{no} = -V_s + \frac{V_d}{2}(2T_{11} - 1) \quad => \quad V_d T_{11} = \frac{V_d}{2} + V_{no} \tag{7.66}$

as V_{no} is the zero sequence component of voltage ,depending upon the modulation scheme it can be chosen to yield different modulating signals. The most generalized expression for V_{no} for three phase networks is as explained in chapter 4. Where V_{no} was obtained by the space vector implementation of the voltage vectors. Expressing the switching functions in terms of their respective modulating signals from Equations 7.62 and 7.64 gives

$$M_{tt} = \frac{2(V_{no})}{V_d} \tag{7.68}$$

$$M_{11} = \frac{2(V_{an} + V_{no})}{V_d} \tag{7.69}$$

$$M_{21} = \frac{2(V_{bn} + V_{no})}{V_d} \tag{7.70}$$

$$M_{31} = \frac{2(V_{cn} + V_{no})}{V_d} \tag{7.71}$$

KCL for the dc link capacitor gives

$$CpV_d = 2(I_s T_{11} - I_a S_{11} - I_b S_{21} - I_c S_{31}) \tag{7.72}$$

$$CpV_\sigma = I_s - I_a - I_b - I_c \tag{7.73}$$

Equations from 7.69 to 7.71 can be written in matrix form as

$$\frac{V_d}{2}\begin{bmatrix} M_{11} \\ M_{21} \\ M_{31} \end{bmatrix} = \begin{bmatrix} V_{an} \\ V_{bn} \\ V_{cn} \end{bmatrix} + \begin{bmatrix} V_{no} \\ V_{no} \\ V_{no} \end{bmatrix} \tag{7.74}$$

Transforming the above matrix into synchronous reference frame (that is the speed with which the motor rotates)

$$\frac{V_d}{2}\begin{bmatrix} m_{qs} \\ m_{ds} \\ m_{os} \end{bmatrix} = \begin{bmatrix} V_{qs} \\ V_{ds} \\ V_{os} \end{bmatrix} + \begin{bmatrix} 0 \\ 0 \\ V_{no} \end{bmatrix} \tag{7.75}$$

$$m_{qs} = \frac{2V_{qs}}{V_d} \tag{7.76}$$

$$m_{ds} = \frac{2V_{ds}}{V_d} \tag{7.77}$$

$$m_{os} = \frac{(2V_{os} + 2V_{no})}{V_d} \tag{7.78}$$

The dc link capacitor equation is written in terms of qdo voltages which is as given in Equation 7.79.

$$CpV_d = (I_s m_{tt} - 1.5i_{qs}m_{qs} - 1.5m_{ds}i_{ds} - 3m_{os}i_{os}) \tag{7.79}$$

since $i_{os} = \frac{i_s}{3}$ the above equation can be written as

$$CpV_d = (I_s(m_{tt} - m_{os}) - 1.5i_{qs}m_{qs} - 1.5m_{ds}i_{ds}) \tag{7.80}$$

Thus from the above equation the fundamental component of the supply current can be written as

$$i_s = CpV_d + 1.5m_{qs}i_{qs} + 1.5m_{ds}i_{ds} \tag{7.81}$$

Equations 7.76 to 7.78 and Equation 7.80 are the basic equations for the design of controller for this converter.

7.5.1 Control Scheme for Converter C

The control objective for this Converter on the line side is to regulate supply current to be in phase with the voltage, and to maintain the dc voltage at a constant value, on the load side speed and flux control are done owing to any change in the load on the machine. The control structure can be explained as, regulation of speed gives the reference command for the q-axis stator current and the regulation of rotor flux gives the reference command for the d-axis stator current. The q-axis and the d-axis currents are compared with the calculated values and the error is processed through a PI controller and using the feedback linearization control technique as explained in the previous chapters, followed by some calculations the reference q and d-axis stator voltages (v_{qs}, v_{ds}) are obtained. When they are normalized by the dc voltage the q and d-axis values (m_{qs} and m_{ds}) of the modulation signals are obtained.

The dc voltage is regulated and the output is used to get the reference magnitude for the supply current, this supply current can be filtered to obtain a pure dc signal, this dc signal is multiplied with the instantaneous phase angle of the supply

voltage this serves as a reference for the supply current. The three phase currents by virtue of the circuit connection contain on-third component of the supply current and so by sensing the three-phase currents and summing them together gives the supply current this current is compared with the reference supply current and the output is used to calculate the zero-sequence voltage v_{os}. The zero sequence voltage is normalized to get m_{os}. The values of m_{qs}, m_{ds} and m_{os} are converted to abc co-ordinates using the frequency calculated by adding the slip speed and the rotor speed. The modulation signals obtained after the transformation are M_{11}, M_{21} and M_{31} which are compared with a high frequency carrier, to obtain the switching pulses for the switching devices and the voltages obtained are applied to the motor.

The modulation signals M_{11}, M_{21} and M_{31} that are the reference commands are the outputs of the controller, reflect those values which when applied to the controller give the desired response for the system. The overall control structure for the Converter B is as given in Figure 7.34.

7.4.2. Simulation Results

The Converter C as shown in Figure 7.33 was simulated using Induction machine similar to the one used for the simulation of the previous converters.
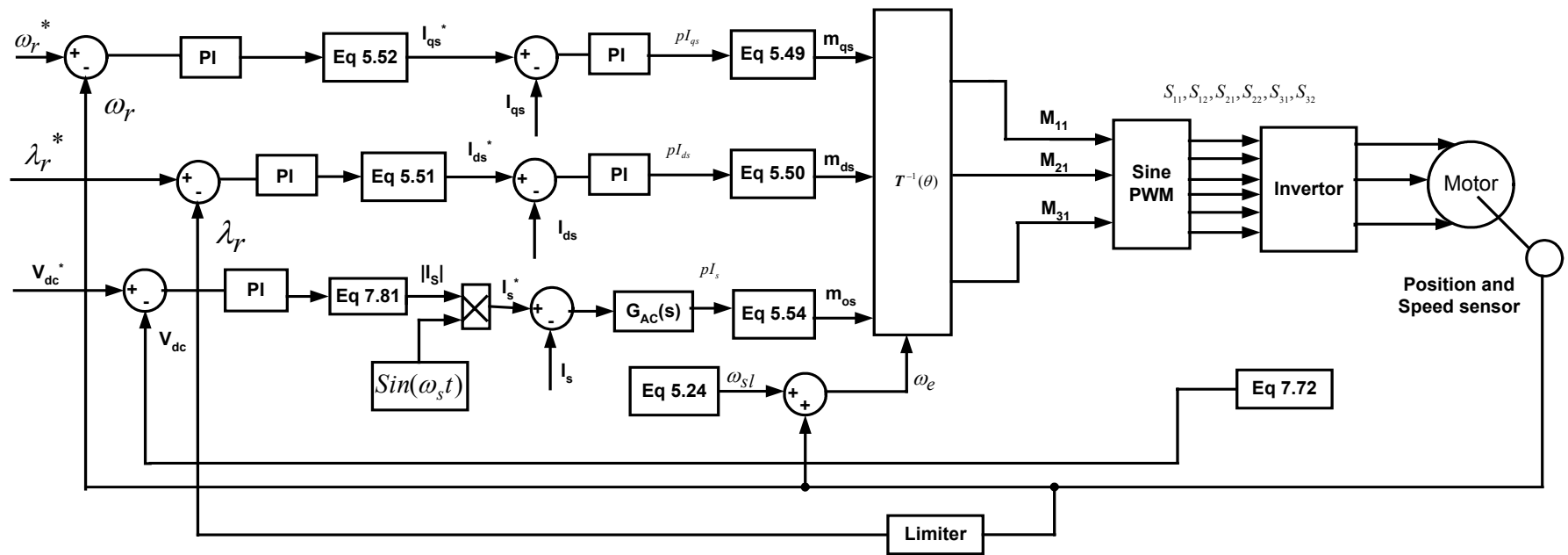
178

Figure 7.34: Control Schematic for converter C

The reference speed for the simulation purpose was ramped up from a zero to the rated motor speed, which was being operated at 33 Hz. For operation above the supply frequency the speed was ramped up from zero to 400 rad/sec; the single-phase supply voltage is 120V at 60 Hz. Figures 7.35 to 7.40 show the simulation results obtained for Converter A for operation below the supply the supply frequency and 7.41 to 7.46 show the simulation results obtained for operation above the supply frequency. Initially the motor was running on no-load and at 1s a load of 4N-m was added on the machine and the system was allowed to settle to a steady state and then the load was removed at 3s.

Figures 7.35 (a) and 7.41(a) show the dc voltage, it can be seen that the voltage reduces slightly when the load is added but it gradually builds up to be constant at its rated value, figures 7.35(b) and 7.41(b) show the supply voltage and current, which are almost in phase with each other. The supply voltage is scaled by some factor so that both the voltage and current can be seen clearly. It can be seen that the dc voltage for this converter is very high when compared to the other topologies due to the fact that the capacitor is the only charging element and supplies voltage to the load. The supply current is not very much balanced due to the fact that the three phases are not symmetric.

Figures 7.36(a), 7.36(b), 7.42(a) and 7.42(b) show the motor frequency and the rotor speed, following any change it can be seen that to keep the rotor speed constant the motor frequency is slightly increased. In Figure 7.36 (c), (d) and 7.42

(c),(d) the slip speed and the electromagnetic torque when a load torque of 4 N-m is added on to the machine is shown.

In Figures 7.37 and 7.43 the rotor flux is shown which follows the command. Figures 7.38 (a) and 7.44(a) show the three-phase actual load currents and Figures 7.38(b) and 7.44 (b) show the plot of load currents after the removal of the component $I_s/3$ versus time.

Figures 7.39 and 7.45 show the unfiltered and the filtered phase voltages. Finally in Figures 7.40 and 7.46 the modulation signals for the three legs are shown.

(a)

(b)
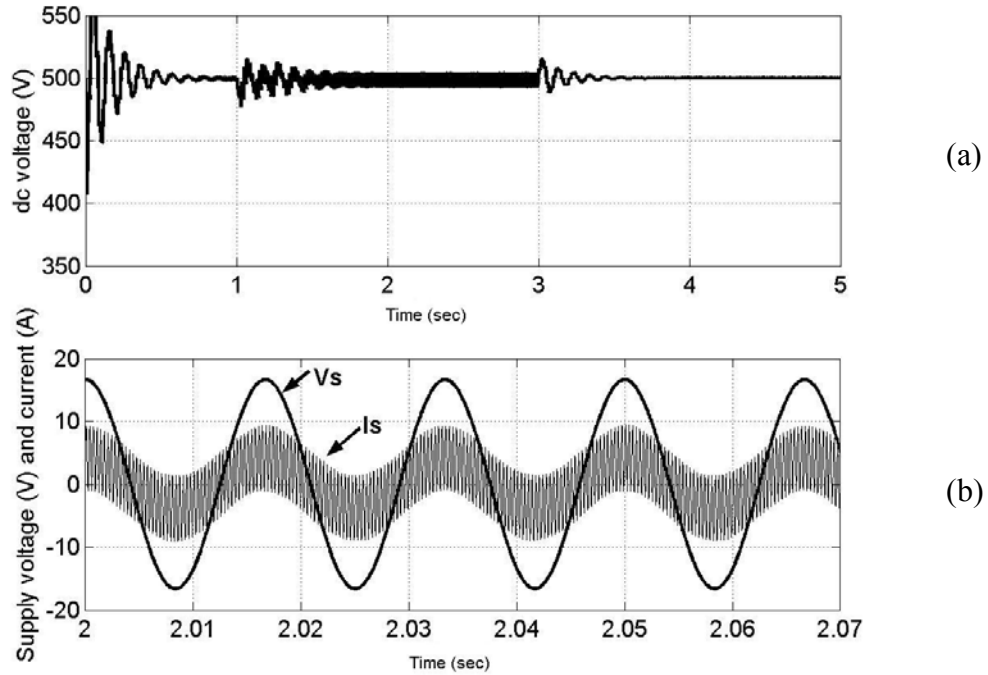
Figure 7.35: Regulated dc voltage, $\omega_r^* = 207\ rad/\sec$ (a) dc voltage regulated at 500V, (b) supply voltage and supply current superimposed on each other.
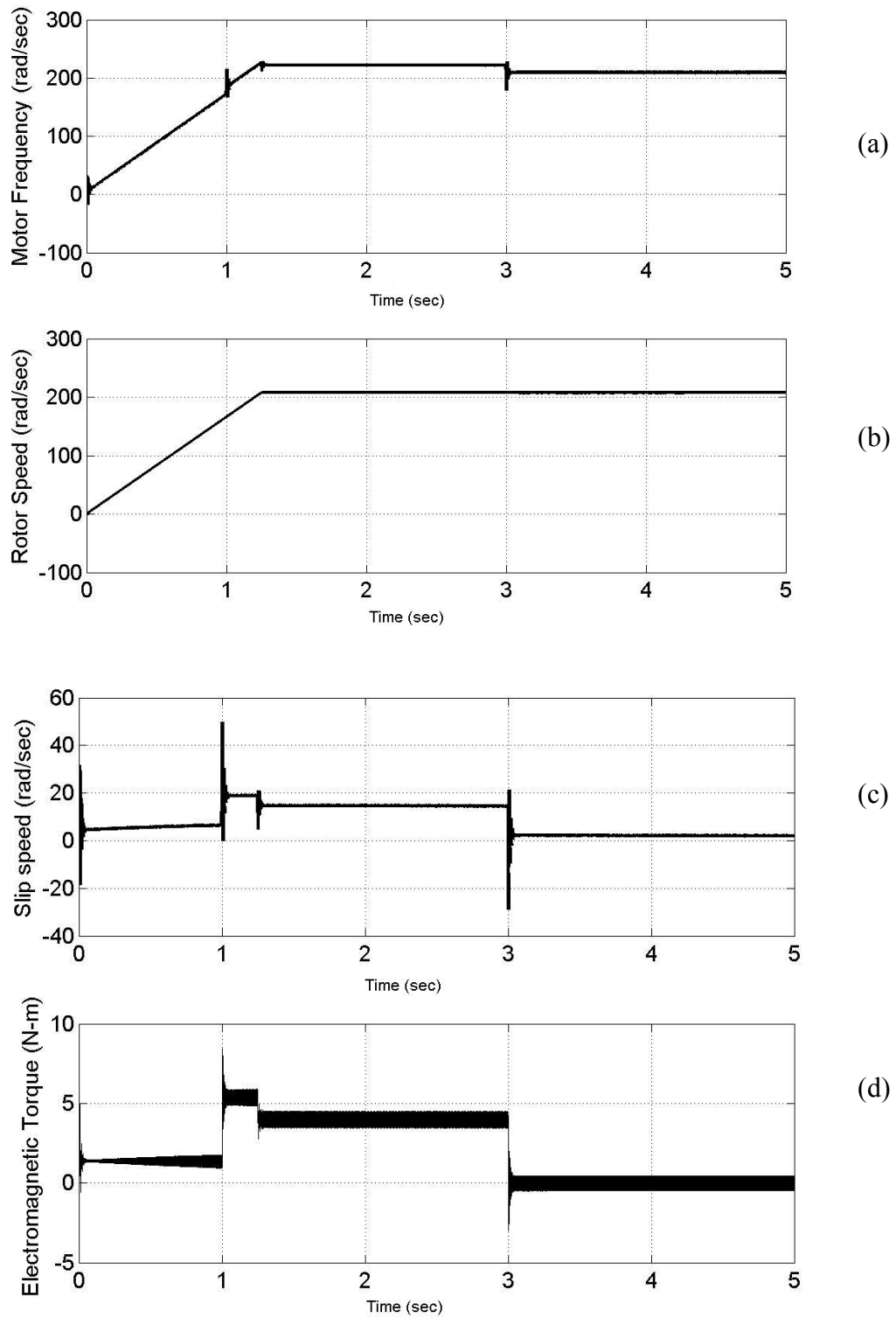
Figure 7.36: Load change, $\omega_r^* = 207\,rad\,/\sec$ (a) The motor frequency in rad/sec, (b) the rotor speed, (c) the slip speed, (d) the electromagnetic torque of 4 N-m.

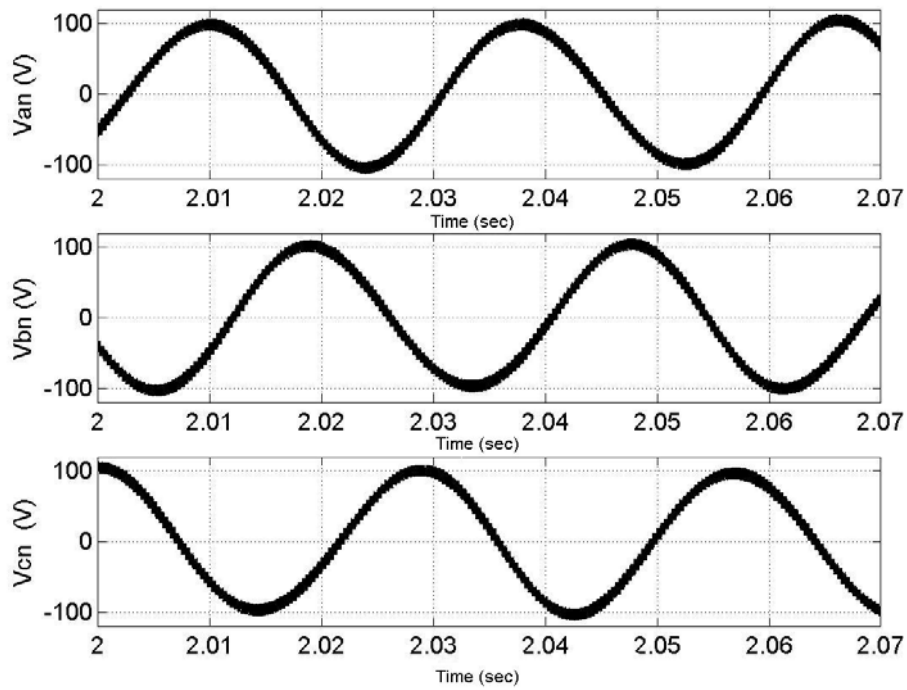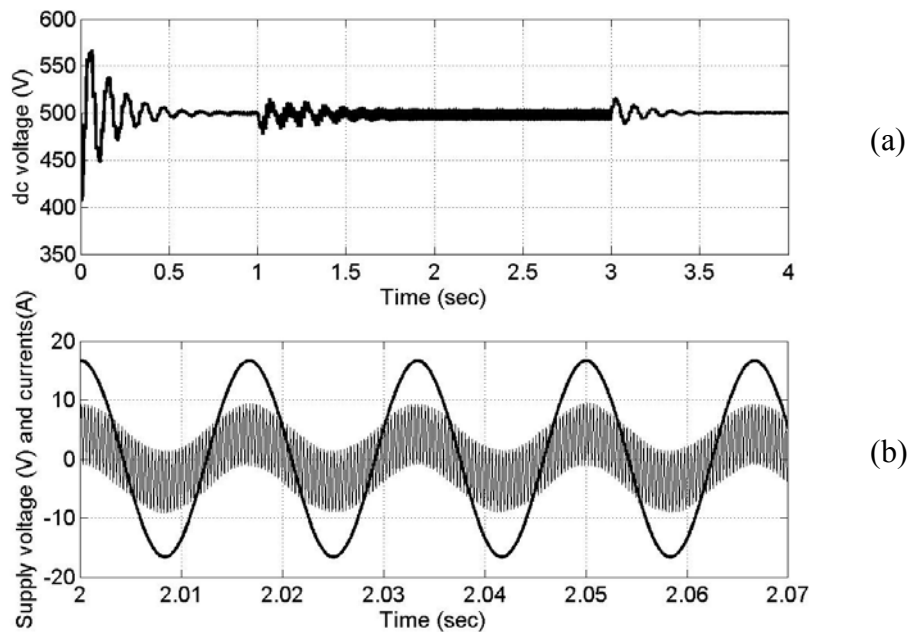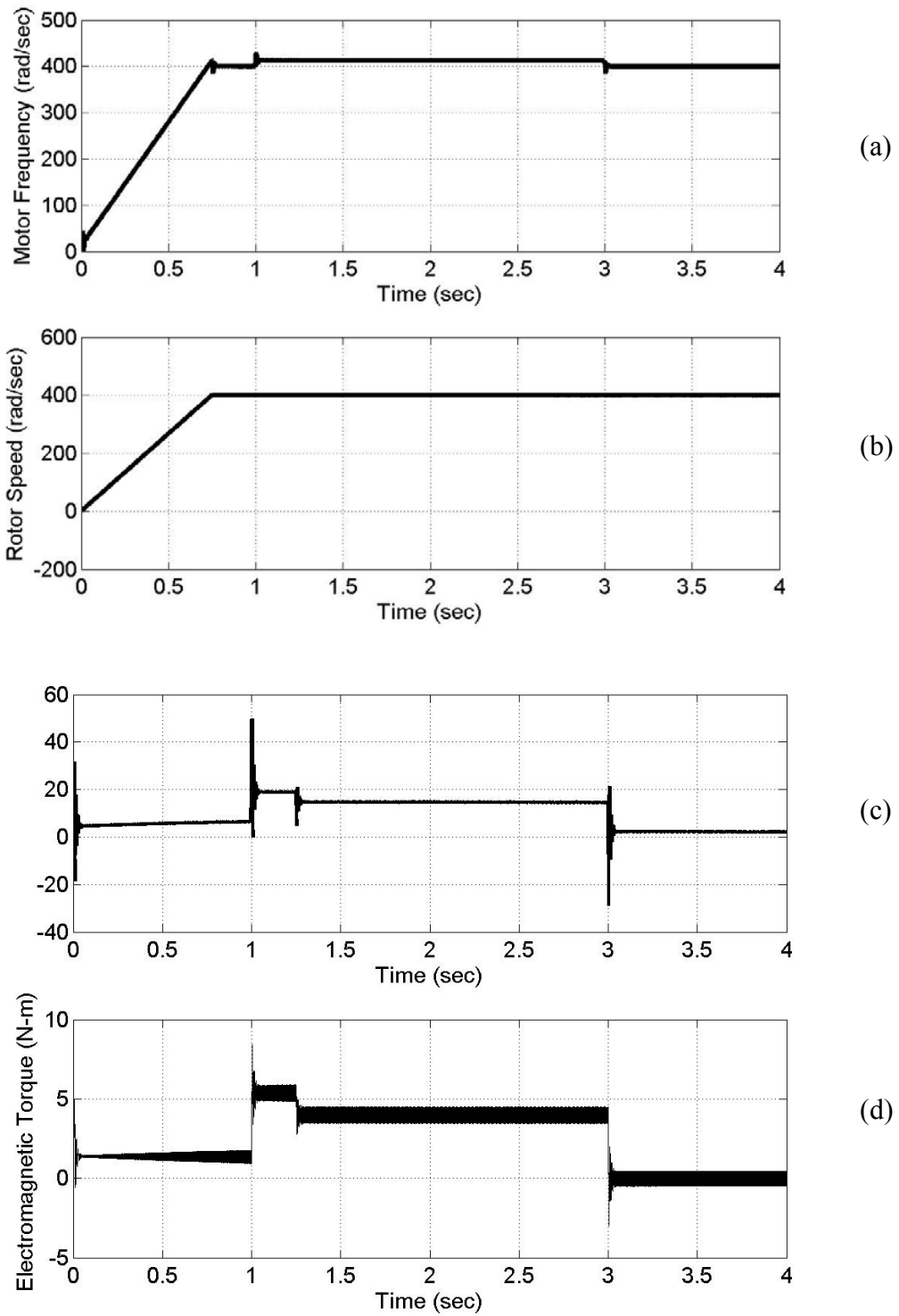Figure 7.37: Rotor flux in Webers, $\omega_r^* = 207\,rad/\sec$.

(a)

(b)
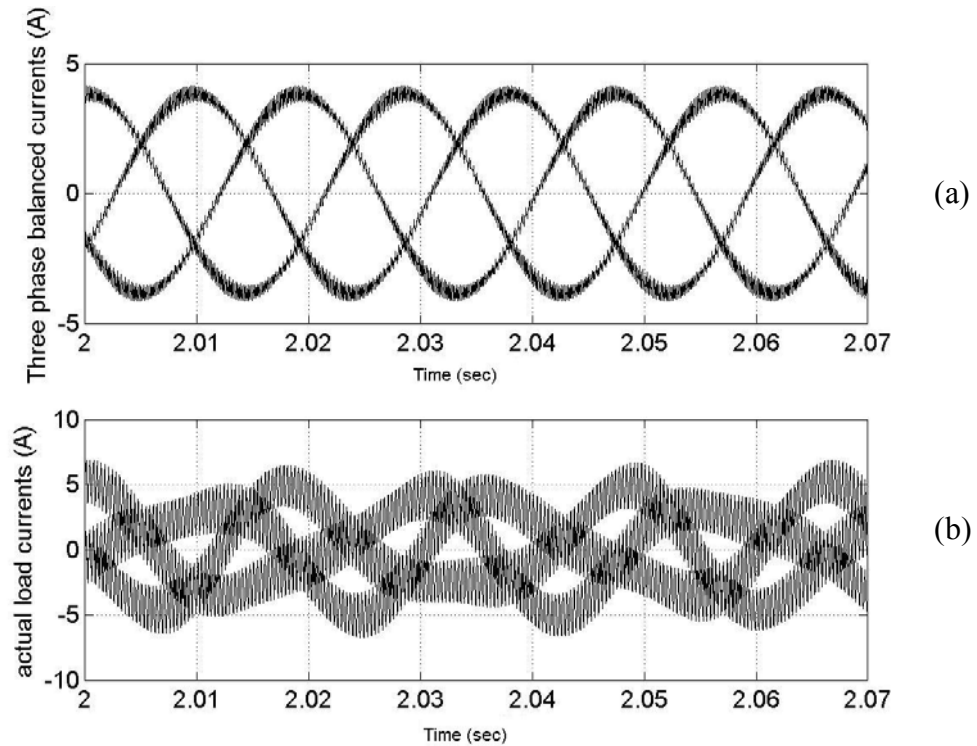
Figure 7.38: On load of 4 N-m, $\omega_r^* = 207\,rad/\sec$ (a) load currents after removal of supply current, (b) the actual load currents

183

Figure 7.39: On load of 4 N- m, $\omega_r^* = 207\,rad/\sec$ (a) the three-phase unfiltered load voltages (V_{an}, V_{bn}, V_{cn}), (b) the three-phase load voltages after filtering the harmonic components.
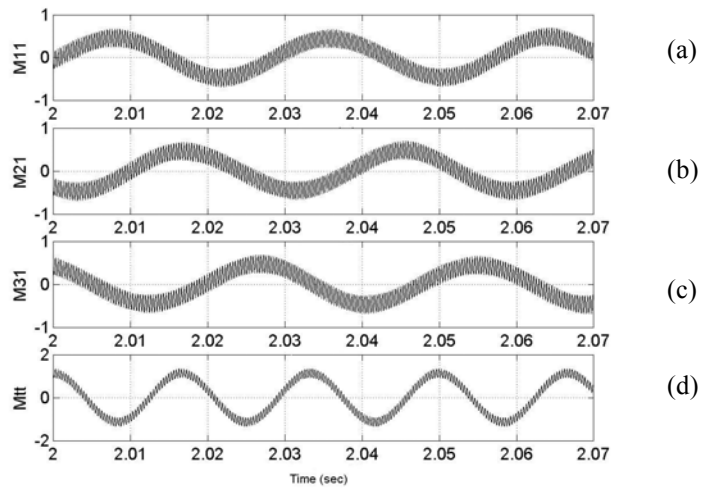
Figure 7.40: Modulation signals, $\omega_r{}^* = 207\,rad/\sec$ (a) M_{11} (b) M_{21} (c) M_{31} (d) M_{tt}.

Operation Above supply frequency:

Figure 7.41: Regulated dc voltage, $\omega_r{}^* = 400\,rad/\sec$ (a) dc voltage regulated at 500V, (b) supply voltage and supply current superimposed on each other.

185

Figure 7.42: Load change, $\omega_r^* = 400\,rad/\sec$ (a) The motor frequency in rad/sec, (b) the rotor speed, (c) the slip speed, (d) the electromagnetic torque of 4 N-m.
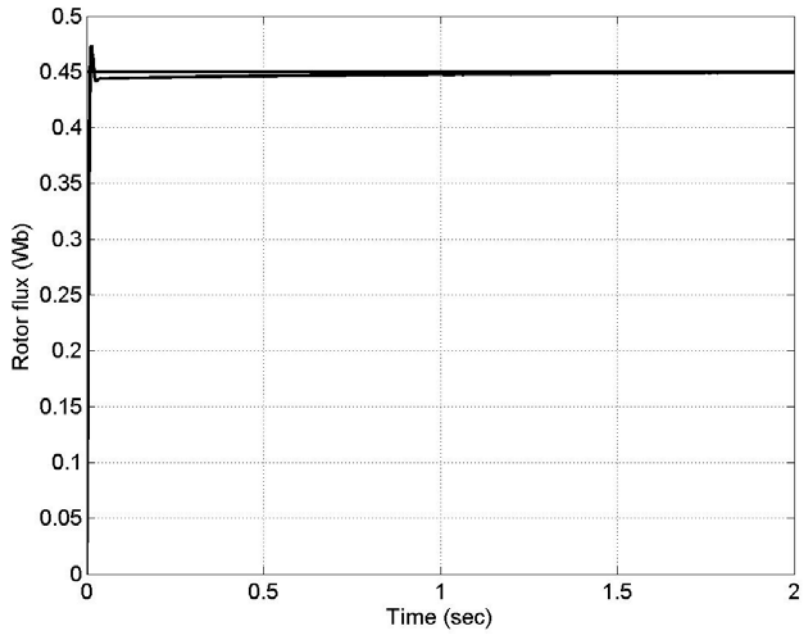
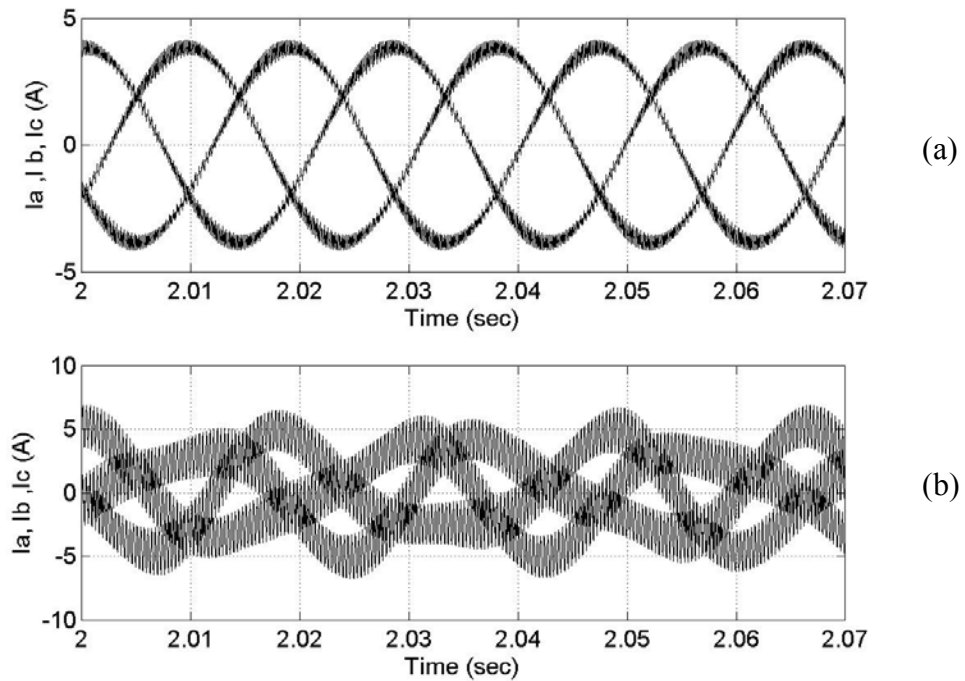Figure 7.43: Rotor flux in Webers, $\omega_r^* = 400\,rad\,/\sec$.

(a)

(b)

Figure 7.44: On load of 4 N-m, $\omega_r^* = 400\,rad\,/\sec$ (a) load currents after removal of supply current, (b) the actual load currents
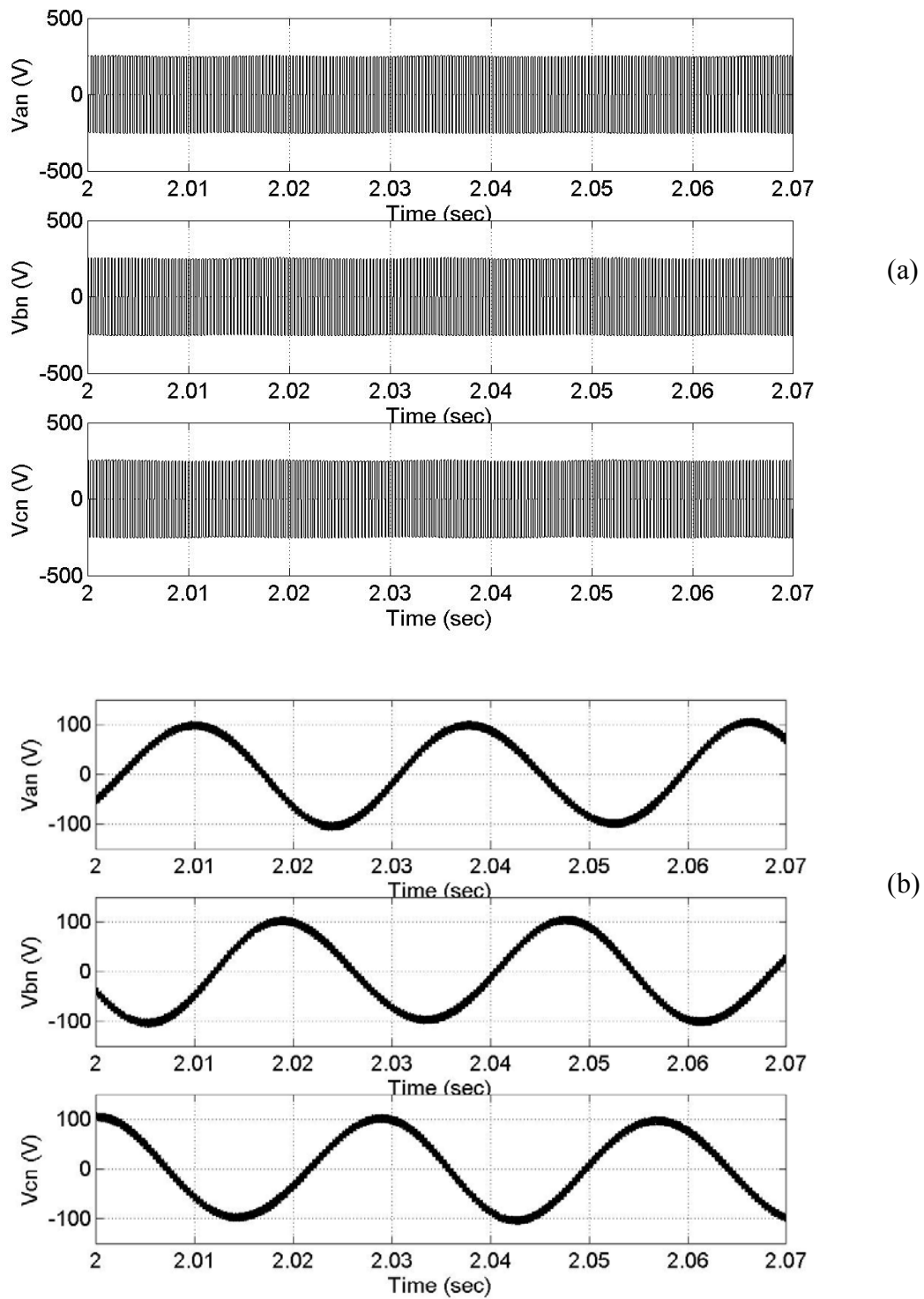
Figure 7.45: On load of 4 N- m, $\omega_r^* = 400\,rad/\sec$ (a) the three-phase unfiltered load voltages (V_{an}, V_{bn}, V_{cn}), (b) the three-phase load voltages after filtering the harmonic components.
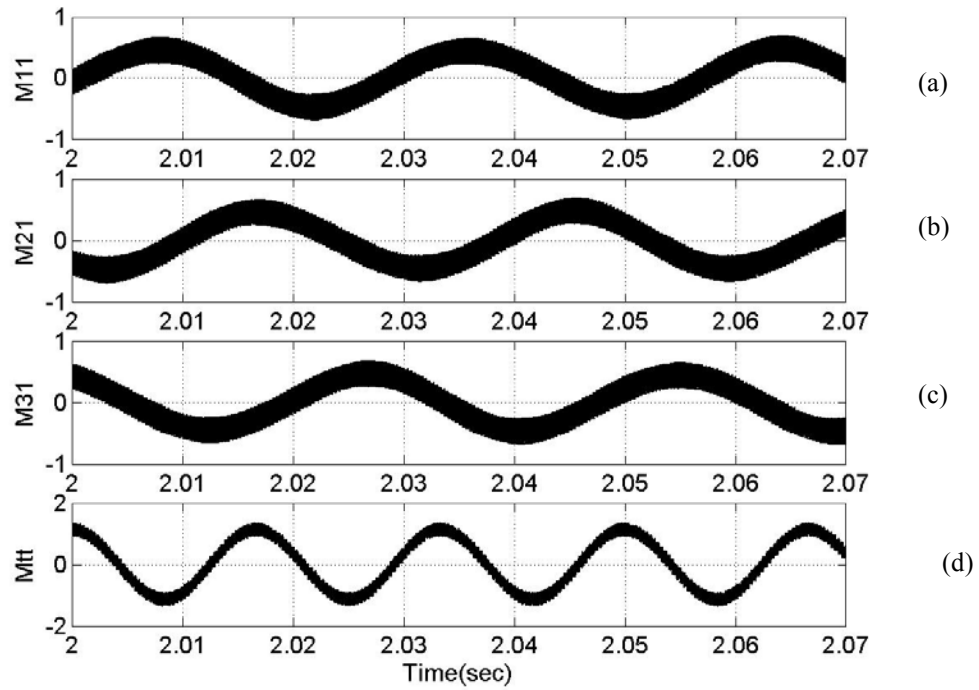
Figure 7.46: Modulation signals, $\omega_r^* = 400\,rad/\sec$ (a) M_{11} (b) M_{21} (c) M_{31} (d) M_{tt}.

In this chapter a detailed analysis of the sparse converters A, B and C, their operation and the dynamic modeling is presented. For the individual converters the control scheme was laid out. The sparse converters fed induction machine was simulated for no-load and on-load conditions. Simulation results to verify the functionality of the converters are shown.